SPECIAL REPORT 99-2

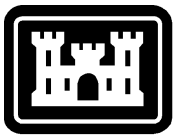

US Army Corps
of Engineers®
Cold Regions Research &
Engineering Laboratory

Effect of Dissolved NaCl on Freezing Curves of Kaolinite, Montmorillonite, and Sand Pastes

S.A. Grant, G.E. Boitnott, and A.R. Tice

January 1999

Abstract: We developed a chemical-thermodynamic procedure for calculating the capillary pressures of aqueous NaCl solutions in a porous medium at temperatures below 0°C by extending the treatment by Brun et al. (1977). Ice in the porous medium was assumed to be a pure phase with thermophysical properties identical to bulk hexagonal ice. The thermophysical properties (and the attendant derivative and integral properties) of the electrolyte solutions were calculated with the Pitzer model as parameterized by Archer (1992).

Experiments were conducted to test this procedure. Pastes of kaolinite clay, montmorillonite, and quartz sand were prepared by washing repeatedly with aqueous solutions of 0.1-, 0.01-, and 0.001-mol kg^{-1} NaCl. The molar unfrozen water contents of these pastes were measured by pulsed nuclear magnetic resonance (NMR) in the temperature range –0.14°C to –66.6°C.

The relationships between ice-solution capillary pressures and specific solution volumes for frozen pastes of each mineral were plotted for all initial solution molalities. While some systemic errors were evident, these plots indicated that the capillary pressure-volume relationships were consistent for pastes of the three minerals and, as expected from theory, unaffected by initial equilibrating solution molality.

How to get copies of CRREL technical publications:

Department of Defense personnel and contractors may order reports through the Defense Technical Information Center:

DTIC-BR SUITE 0944
8725 JOHN J KINGMAN RD
FT BELVOIR VA 22060-6218
Telephone 1 800 225 3842
E-mail help@dtic.mil
msorders@dtic.mil
WWW http://www.dtic.dla.mil/

All others may order reports through the National Technical Information Service:

NTIS
5285 PORT ROYAL RD
SPRINGFIELD VA 22161
Telephone 1 800 553 6847 or 1 703 605 6000
1 703 487 4639 (TDD for the hearing-impaired)
E-mail orders@ntis.fedworld.gov
WWW http://www.ntis.gov

A complete list of all CRREL technical publications is available from:

USACRREL (CECRL-IB)
72 LYME RD
HANOVER NH 03755-1290
Telephone 1 603 646 4338
E-mail techpubs@crrel.usace.army.mil

For information on all aspects of the Cold Regions Research and Engineering Laboratory, visit our World Wide Web site: http://www.crrel.usace.army.mil

Special Report 99-2

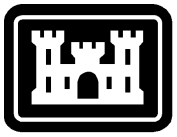

US Army Corps of Engineers®
Cold Regions Research & Engineering Laboratory

Effect of Dissolved NaCl on Freezing Curves of Kaolinite, Montmorillonite, and Sand Pastes

S.A. Grant, G.E. Boitnott, and A.R. Tice

January 1999

Prepared for
OFFICE OF THE CHIEF OF ENGINEERS
STRATEGIC ENVIRONMENTAL RESEARCH AND DEVELOPMENT PROGRAM
DEPARTMENT OF ENERGY

PREFACE

This report was written by Dr. Steven A. Grant, Research Physical Scientist, and Ginger E. Boitnott, Physical Science Technician, Geochemical Science Division, Research and Engineering Directorate, of the U.S. Army Cold Regions Research and Engineering Laboratory, Hanover, New Hampshire, and Andrew R. Tice, formerly of CRREL.

The report was funded by DOD contract no. 4A161102AT24, *Research in Snow, Ice, and Frozen Ground*, Task SC, *Frozen Ground Processes*, Work Unit F02, *Chemical Processes in Frozen Ground*; the Strategic Environmental Research and Development Program (SERDP); and DOE Interagency Agreement no. DE-AI05-940R22141. The report was technically reviewed by Karen Henry of CRREL and T.E. Osterkamp of the University of Alaska Fairbanks.

The authors thank Dr. D.G. Archer, Division of Kinetics and Chemical Thermodynamics, National Institute of Standards and Technology, Gaithersburg, Maryland, for providing the computer program he wrote to calculate the thermophysical properties of NaCl(aq) and H_2O(l) from his parameterization of the Pitzer model. They also thank Ms. S.E. Hardy for reviewing this report in manuscript form.

CONTENTS

Page

Preface ii
Nomenclature v
Introduction 1
Theory 2
    Gibbs–Duhem equations 2
    Kelvin equations 2
    Systems with pure liquid-water phases 2
    Systems with aqueous-electrolyte-solution liquid phases 4
    Relationship of capillary pressures to pore radii and liquid-water contents 5
Materials and methods 5
    Sample preparation 5
    Experimental procedures 6
Experimental results 7
Comparison with theory 10
    Calculation of the necessary thermophysical properties 10
    Plots of capillary pressures against liquid specific volumes 20
Conclusion 24
Literature cited 24
Appendix A: Effect of concentration scales on activities 27
Abstract 29

ILLUSTRATIONS

Figure Page

1. Unfrozen water contents, as measured by pulsed NMR, of freezing kaolinite pastes cooled from 0°C to –66.6°C 11
2. Unfrozen water contents, as measured by pulsed NMR, of freezing kaolinite pastes warmed from –66.6°C to 0°C 11
3. Unfrozen water contents, as measured by pulsed NMR, of freezing montmorillonite pastes cooled from 0°C to –66.6°C 11
4. Unfrozen water contents, as measured by pulsed NMR, of freezing montmorillonite pastes warmed from –66.6°C to 0°C 12
5. Unfrozen water contents, as measured by pulsed NMR, of freezing sand pastes cooled from 0°C to –66.6°C 12
6. Unfrozen water contents, as measured by pulsed NMR, of freezing sand pastes warmed from –66.6°C to 0°C 13
7. Constant-pressure heat capacity of H_2O(cr,I) under p = 0.101325 MPa and T = 200 K to 268 K 14
8. Constant-pressure heat capacity of H_2O(l) and H_2O(cr,I) under p = 0.101325 MPa and T = 200 K to 300 K 16
9. Relationships between unfrozen-solution specific volumes and ice-solution capillary pressures for kaolinite pastes cooled from 0°C to –66.6°C 21

10. Relationships between unfrozen-solution specific volumes and ice-solution capillary pressures for kaolinite pastes warmed from –66.6°C to 0°C 22
11. Relationships between unfrozen-solution specific volumes and ice-solution capillary pressures for montmorillonite pastes cooled from 0°C to –66.6°C 22
12. Relationships between unfrozen-solution specific volumes and ice-solution capillary pressures for montmorillonite pastes warmed from –66.6°C to 0° 23
13. Relationships between unfrozen-solution specific volumes and ice-solution capillary pressures for sand pastes cooled from 0°C to –66.6°C 23
14. Relationships between unfrozen-solution specific volumes and ice-solution capillary pressures for sand pastes warmed from –66.6°C to 0°C 24

TABLES

Table Page
1. Equilibrating solution molalities and total specific water masses for pastes frozen then thawed in this study 7
2. Unfrozen-water contents, as measured by pulsed NMR, of kaolinite pastes cooled from 0°C to –66.6°C 7
3. Unfrozen-water contents, as measured by pulsed NMR, of kaolinite pastes warmed from –66.6°C to 0°C 8
4. Unfrozen-water contents, as measured by pulsed NMR, of montmorillonite pastes cooled from 0°C to –66.6°C 8
5. Unfrozen-water contents, as measured by pulsed NMR, of montmorillonite pastes warmed from –66.6°C to 0°C 9
6. Unfrozen-water contents, as measured by pulsed NMR, of sand pastes cooled from 0°C to –66.6°C 9
7. Unfrozen-water contents, as measured by pulsed NMR, of sand pastes warmed from –66.6°C to 0°C 10
8. Coefficients to Speedy's (1987) empirical equations for calculating the thermophysical properties of supercooled water 16

NOMENCLATURE

Symbol	*Definition*	*SI unit*	*Eq. first cited*
$a_{\pm\mathrm{NaCl(aq)}}$	mean-ionic activity of NaCl(aq)	dimensionless	59
$a_{m,\mathrm{B}}$	activity of solute B (molality concentration scale)	dimensionless	66
$a_{x,\mathrm{B}}$	activity of solute B (mole-fraction concentration scale)	dimensionless	67
A_{C}	Debye–Hückel coefficient for apparent molar constant-pressure heat capacity	$\mathrm{J\,K^{-1}\,mol^{-1}}$	46
$A^{\mathrm{sg}}_{\mathrm{s,m}}$	molar area of solid / gas interface	$\mathrm{m^2\,mol^{-1}}$	3
$A^{\mathrm{ls}}_{\mathrm{s,m}}$	molar area of liquid / solid interface	$\mathrm{m^2\,mol^{-1}}$	3
a	fitted coefficient in Maier–Kelly equation	$\mathrm{J\,K^{-1}\,mol^{-1}}$	33
b	fitted coefficient in Maier–Kelly equation	$\mathrm{J\,K^{-2}\,mol^{-1}}$	33
b	a constant equal to 1.2	$\mathrm{kg^{1/2}\,mol^{-1/2}}$	46
$B^{(\mathrm{n})}_{C_p}$	parameter in Speedy's equation	$\mathrm{J\,mol^{-1}}$	42
c	fitted coefficient in Maier–Kelly equation	$\mathrm{J\,K\,mol^{-1}}$	33
$C^{(0)}_{\mathrm{NaCl}}$	ion-interaction parameter of Pitzer model	$\mathrm{kg^2\,mol^{-2}}$	48
$C^{(1)}_{\mathrm{NaCl}}$	ion-interaction parameter of Pitzer model	$\mathrm{kg^2\,mol^{-2}}$	48
C_p	constant-pressure heat capacity	$\mathrm{J\,K^{-1}}$	42
$C_{p,\mathrm{m}}$	constant-pressure molar heat capacity of the solution	$\mathrm{J\,K^{-1}\,mol^{-1}}$	44
$C^{\ominus}_{p,\mathrm{H_2O(l)}}$	constant-pressure standard-state heat capacity of liquid water	$\mathrm{J\,K^{-1}\,mol^{-1}}$	44
$C_p(m_r)$	constant-pressure heat capacity of a solution with a molality equal to m_{r}	$\mathrm{J\,K^{-1}\,mol^{-1}}$	46
C_{C_p}	parameter in Speedy's equation	$\mathrm{J\,mol^{-1}}$	42
I_m	molality-based ionic strength	$\mathrm{mol\,kg^{-1}}$	46
I_r	molality-based ionic strength of the reference solution	$\mathrm{mol\,kg^{-1}}$	46
m	molal concentration of the solute	$\mathrm{mol\,kg^{-1}}$	46
m_{i}	initial NaCl molality of solutions of pastes	$\mathrm{mol\,kg^{-1}}$	22
$m_{T_{\mathrm{f}}}$	NaCl molality of solutions of pastes at $T = T_{\mathrm{f}}$	$\mathrm{mol\,kg^{-1}}$	22
m_r	reference molality	$\mathrm{mol\,kg^{-1}}$	46
$m_{\pm\mathrm{NaCl(aq)}}$	mean-ionic molality NaCl in an aqueous solution	$\mathrm{mol\,kg^{-1}}$	59
$m^{\ominus}_{\pm\mathrm{NaCl(aq)}}$	standard-state mean-ionic molality of NaCl	$\mathrm{mol\,kg^{-1}}$	59
n_T	total number of molecules in a mixture or solution	mol	36
n_{A}	number of molecules of component A in a mixture or solution	mol	36
$n_{\mathrm{H_2O(l)}}$	amount of water in the solution	mol	44
$n_{\mathrm{NaCl(aq)}}$	amount of NaCl in the solution	mol	44
p	pressure	Pa	1

p^{g}	pressure of gas phase	Pa	1
p^{l}	pressure of liquid phase	Pa	1
p^{s}	pressure of solid phase	Pa	1
p_c	capillary pressure	Pa	11
R	gas constant (= 8.314 510 70)	J K^{-1} mol^{-1}	40
S_m^{g}	molar entropy of gas phase	J K^{-1} mol^{-1}	1
S_{m,H_2O}^{*g}	molar entropy of a pure water vapor	J K^{-1} mol^{-1}	4
S_{m,H_2O}^{*l}	molar entropy of a pure water liquid	J K^{-1} mol^{-1}	5
S_{m,H_2O}^{*s}	molar entropy of a pure water ice	J K^{-1} mol^{-1}	6
S_m^{l}	molar entropy of liquid phase	J K^{-1} mol^{-1}	1
S_m^{s}	molar entropy of solid phase	J K^{-1} mol^{-1}	1
T	thermodynamic temperature	K	1
T_0	bulk solvent melting point for a given solution composition	K	13
T_s	apparent limiting temperature for supercooled water = 227.15 K	K	42
V_m^{g}	molar volume of gas phase	m^3	1
V_m^{l}	molar volume of liquid phase	m^3	1
V_m^{s}	molar volume of solid phase	m^3	1
V_{m,H_2O}^{*g}	molar volume of pure-water vapor	m^3	4
V_{m,H_2O}^{*l}	molar volume of pure-water liquid phase	m^3	5
V_{m,H_2O}^{*s}	molar volume of pure-water ice	m^3	6
$x_{NaCl(aq)}^{\alpha}$	mole fraction of B in the α phase	dimensionless	1
z_{Na}	charge number of Na^+ cation	dimensionless	46
z_{Cl}	charge number of Cl^- anion	dimensionless	46
α	constant in Pitzer model	kg$^{-1/2}$ mol$^{-1/2}$	47
α_2	constant in Pitzer model (as revised by Archer)	kg$^{-1/2}$ mol$^{-1/2}$	48
$\beta_{NaCl}^{(0)}$	ion-interaction parameter of Pitzer model	kg mol^{-1}	47
$\beta_{NaCl}^{(1)}$	ion-interaction parameter of Pitzer model	kg mol^{-1}	47
$\Delta_s^{l} H_{m,H_2O}^{*}$	molar enthalpy of melting for pure water	J mol^{-1}	31
γ^{ls}	liquid–solid interfacial tension	N m^{-1}	3
γ^{sg}	solid–gas interfacial tension	N m^{-1}	3
$\gamma_{\pm NaCl(aq)}$	mean-ionic activity coefficient for NaCl in an aqueous solution	dimensionless	59
ε	reduced temperature $\equiv \dfrac{T - T_s}{T_s}$	dimensionless	42
μ_B^{α}	chemical potential of B in the α phase	J mol^{-1}	1
$\mu_{m,B}^{\ominus}$	standard-state chemical potential of solute B (molality concentration scale)	J mol^{-1}	60
$\mu_{x,B}^{\ominus}$	standard-state chemical potential of solute B (mole-fraction concentration scale)	J mol^{-1}	61
ν	$= \nu_{Na} + \nu_{Cl}$	dimensionless	46

ν_{Cl}	stoichiometric number of Cl in NaCl	dimensionless	46
ν_{Na}	stoichiometric number of Na in NaCl	dimensionless	46
θ_i	initial specific liquid-water content	kg kg^{-1}	22
θ_{T_f}	specific liquid-water content at $T = T_f$	kg kg^{-1}	22
θ	superscript indicating a standard substance		38
*	superscript indicating a pure substance		4
∞	superscript indicating a solution at infinite dilution		60

Effect of Dissolved NaCl on Freezing Curves of Kaolinite, Montmorillonite, and Sand Pastes

S.A. GRANT, G.E. BOITNOTT, AND A.R. TICE

INTRODUCTION

Chemical thermodynamics has long been used to calculate the heaving pressures and liquid-water contents of frozen ground (Everett 1961, Defay and Prigogine 1966). In most instances, the effects of solutes in the liquid phase have been neglected in the application of chemical–thermodynamic theory to frozen porous media: the liquid phases are typically assumed to be pure. At equilibrium, ice accepts few solutes and these at only vanishingly small mole fractions. Most solutes in frozen ground are in the liquid phase (Hobbs 1974). At temperatures appreciably below 0°C, where most of the water in a water–electrolyte system is in the ice phase, liquid solutions tend to be highly concentrated. In these environments, the effects of solutes on the freezing behavior of ground can be considerable.

In recent years, theoretical and experimental advances have provided the tools for estimating the thermophysical properties of aqueous electrolyte solutions at subzero temperatures. The major theoretical advance has been the development and acceptance of the Pitzer model of electrolyte solutions (Pitzer 1991). The Pitzer model allows for the calculation of the important physiochemical properties of simple and complex aqueous electrolyte solutions over a wide range of temperatures, pressures, and compositions. Most importantly for this discussion, the Pitzer model allows the accurate estimation of electrolyte-solution properties at subzero temperatures (Spencer et al. 1990, Archer 1992, Marion and Grant 1994). Since many of the thermophysical properties modelled by the Pitzer model are relative to the same properties of the solvent, a critical component when modelling the thermophysical properties of electrolyte solutions is accurate measurements of pure-solvent properties. Historically, this has presented problems for water at temperatures below its equilibrium freezing point. Novel experimental procedures have allowed the heat capacity and density of supercooled liquid water to be measured accurately at temperatures as low as –35°C (Angell et al. 1973, Hare and Sorensen 1987). Speedy (1987) has fitted much of the available data on supercooled water to a family of equations that calculate physical–chemical properties of liquid water under atmospheric pressure in the temperature range 0 to –45°C.

To our knowledge, no one has applied these new capabilities to the long-standing problem of calculating the effects of solutes on the freezing curves of frozen ground. The objectives of the research presented here were:

1. To extend the conventional (i.e., pure-phase) chemical–thermodynamic theory of frozen ground to the liquid phases of aqueous electrolyte solutions
2. To calculate the needed chemical–thermodynamic data from physical–chemical models of ice, water, and electrolyte solutions
3. To make experimental measurements of liquid-water contents of sand and clay-mineral pastes with which to test this extension of the model.

In this report, we initially discuss the chemical–thermodynamic methods by which capillary pressures of either pure or solution liquid phases can be calculated for frozen porous media. The thermophysical data needed to make these calculations are presented. We then describe and evaluate the data from a set of experiments we conducted to test this approach to calculating capillary pressures.

THEORY

Here we follow closely the lucid, complete presentation of the chemical–thermodynamic theory of frozen porous media presented by Brun et al. (1977). Consider three phases, solid (s), liquid (l), and gas (g), which are in thermal, but not necessarily hydrostatic, equilibrium [i.e., $T^{s} = T^{l} = T^{g} = T$, but $p^{s} \neq p^{l} \neq p$, where T is temperature (K) and p is pressure (Pa)]. Their development begins with two sets of classic equalities:

1. The Gibbs–Duhem equations, and

2. The Kelvin equations.

Gibbs–Duhem equations

For each phase, the Gibbs–Duhem relation holds:

$$\begin{aligned} 0 &= S_{m}^{g}\,dT - V_{m}^{g}\,dp^{g} + \sum_{B} x_{B}^{g}\,d\mu_{B}^{g} \\ 0 &= S_{m}^{l}\,dT - V_{m}^{l}\,dp^{l} + \sum_{B} x_{B}^{l}\,d\mu_{B}^{l} \\ 0 &= S_{m}^{s}\,dT - V_{m}^{s}\,dp^{s} + \sum_{B} x_{B}^{s}\,d\mu_{B}^{s} \end{aligned} \tag{1}$$

where S_{m}^{g}, S_{m}^{l}, and S_{m}^{s} are the molar entropies (J K^{-1} mol^{-1}) of the gas, liquid, and solid phases, respectively; V_{m}^{s}, V_{m}^{l}, and V_{m}^{s}, their molar volumes (m^{3} mol^{-1}); x_{B}^{g}, x_{B}^{l}, and x_{B}^{s}, the mole fraction of component B in the three phases; and μ_{B}^{g}, μ_{B}^{l}, and μ_{B}^{s}, the chemical potentials (J mol^{-1}) of component B in the three phases.

Kelvin equations

The Kelvin equations give the pressure gradients across the gas / solid and liquid / solid interfaces in terms of the differential geometry of these interfaces:

$$p^{g} - p^{s} = \gamma^{sg}\,\frac{dA_{s,m}^{sg}}{dV_{m}^{g}} \tag{2}$$

$$p^{l} - p^{s} = \gamma^{ls}\,\frac{dA_{s,m}^{lg}}{dV_{m}^{l}} \tag{3}$$

where $A_{s,m}^{ls}$ and $A_{s,m}^{sg}$ (m^{2} mol^{-1}) are the molar areas of the liquid / solid and solid / gas interfaces, respectively, and γ^{ls} and γ^{sg} (N m^{-1}) are the corresponding interfacial tensions.

Capillary pressures of liquid phases can be estimated by applying these equalities. Below we present a summary of the development: first for systems with pure-water liquid phases, then for aqueous-electrolyte-solution liquid phases.

Systems with pure liquid-water phases

If the solid, liquid, and vapor phases are pure, then eq 1 can be rewritten:

$$0 = S_{m,H_2O}^{*g}\,dT - V_{m,H_2O}^{*g}\,dp^{g} + d\mu_{H_2O}^{*g} \tag{4}$$

$$0 = S_{m,H_2O}^{*l}\,dT - V_{m,H_2O}^{*l}\,dp^{l} + d\mu_{H_2O}^{*l} \tag{5}$$

$$0 = S_{m,H_2O}^{*s}\,dT - V_{m,H_2O}^{*s}\,dp^{s} + d\mu_{H_2O}^{*s} \tag{6}$$

where the superscript * indicates a pure phase. By taking the partial derivatives of eq 2 and 3, dp^{g} and dp^{l} can be related to dp^{s} by:

$$\mathrm{d}p^{\mathrm{g}} = \mathrm{d}p^{\mathrm{s}} + \mathrm{d}\left(\gamma^{\mathrm{sg}}\frac{\mathrm{d}A^{\mathrm{sg}}_{\mathrm{s,m}}}{\mathrm{d}V^{\mathrm{g}}_{\mathrm{m}}}\right) \tag{7}$$

and

$$\mathrm{d}p^{\mathrm{l}} = \mathrm{d}p^{\mathrm{s}} + \mathrm{d}\left(\gamma^{\mathrm{ls}}\frac{\mathrm{d}A^{\mathrm{ls}}_{\mathrm{s,m}}}{\mathrm{d}V^{\mathrm{l}}_{\mathrm{m}}}\right). \tag{8}$$

By subtracting eq 4 from eq 6 and eq 6 from eq 5, then subtracting the latter difference from the former, the following relation is obtained after rearrangement:

$$\left(\frac{S^{*\mathrm{s}}_{\mathrm{m},\mathrm{H_2O}} - S^{*\mathrm{g}}_{\mathrm{m},\mathrm{H_2O}}}{V^{*\mathrm{s}}_{\mathrm{m},\mathrm{H_2O}} - V^{*\mathrm{g}}_{\mathrm{m},\mathrm{H_2O}}} - \frac{S^{*\mathrm{l}}_{\mathrm{m},\mathrm{H_2O}} - S^{*\mathrm{s}}_{\mathrm{m},\mathrm{H_2O}}}{V^{*\mathrm{l}}_{\mathrm{m},\mathrm{H_2O}} - V^{*\mathrm{s}}_{\mathrm{m},\mathrm{H_2O}}}\right)\mathrm{d}T$$

$$= \frac{V^{*\mathrm{g}}_{\mathrm{m},\mathrm{H_2O}}}{V^{*\mathrm{g}}_{\mathrm{m},\mathrm{H_2O}} - V^{*\mathrm{s}}_{\mathrm{m},\mathrm{H_2O}}}\mathrm{d}\left(\gamma^{\mathrm{sg}}\frac{\mathrm{d}A^{\mathrm{sg}}_{\mathrm{s,m}}}{\mathrm{d}V^{\mathrm{g}}_{\mathrm{m}}}\right) \tag{9}$$

$$- \frac{V^{*\mathrm{l}}_{\mathrm{m},\mathrm{H_2O}}}{V^{*\mathrm{l}}_{\mathrm{m},\mathrm{H_2O}} - V^{*\mathrm{s}}_{\mathrm{m},\mathrm{H_2O}}}\mathrm{d}\left(\gamma^{\mathrm{ls}}\frac{\mathrm{d}A^{\mathrm{ls}}_{\mathrm{s,m}}}{\mathrm{d}V^{\mathrm{l}}_{\mathrm{m}}}\right).$$

By noting that $V^{*\mathrm{g}}_{\mathrm{m},\mathrm{H_2O}} >> V^{*\mathrm{l}}_{\mathrm{m},\mathrm{H_2O}}$ and by assuming that $\gamma^{\mathrm{sg}}\frac{\mathrm{d}A^{\mathrm{sg}}_{\mathrm{s,m}}}{\mathrm{d}V^{\mathrm{g}}_{\mathrm{m}}} = 0$, the following relation is obtained:

$$\left(S^{*\mathrm{l}}_{\mathrm{m},\mathrm{H_2O}} - S^{*\mathrm{s}}_{\mathrm{m},\mathrm{H_2O}}\right)\mathrm{d}T = V^{*\mathrm{l}}_{\mathrm{m},\mathrm{H_2O}}\mathrm{d}\left(\gamma^{\mathrm{ls}}\frac{\mathrm{d}A^{\mathrm{ls}}_{\mathrm{s,m}}}{\mathrm{d}V^{\mathrm{l}}_{\mathrm{m}}}\right). \tag{10}$$

By defining capillary pressure (Pa), p_c, as

$$p_{\mathrm{c}} = p^{\mathrm{l}} - p^{\mathrm{s}}, \tag{11}$$

it can be seen from eq 8 and 11 that

$$\mathrm{d}p_{\mathrm{c}} = \mathrm{d}\left(\gamma^{\mathrm{ls}}\frac{\mathrm{d}A^{\mathrm{ls}}_{\mathrm{s,m}}}{\mathrm{d}V^{\mathrm{l}}_{\mathrm{m}}}\right). \tag{12}$$

Therefore, the capillary pressure of liquid water in a frozen porous medium can be calculated by

$$\int_0^{p_{\mathrm{c}}}\mathrm{d}p_{\mathrm{c}} \equiv p_{\mathrm{c}} = \int_{T_0}^{T}\frac{S^{*\mathrm{l}}_{\mathrm{m},\mathrm{H_2O}} - S^{*\mathrm{s}}_{\mathrm{m},\mathrm{H_2O}}}{V^{*\mathrm{l}}_{\mathrm{m},\mathrm{H_2O}}}\,\mathrm{d}T \tag{13}$$

where T_0 (K) is the melting point of the bulk liquid phase.

To evaluate the righthand side of eq 13, the following properties must be measured or estimated for all temperatures of interest:

1. The melting point of the liquid phase in bulk
2. Entropy of the liquid phase
3. Entropy of the ice phase
4. Molar volume of the liquid phase.

Systems with aqueous-electrolyte-solution liquid phases

The treatment presented in the previous section can be extended directly to electrolyte–H_2O systems. For example, eq 1 for a NaCl–H_2O system can be written

$$0 = S^{*g}_{m,H_2O}\,dT - V^{*g}_{m,H_2O}\,dp^g + d\mu^{*g}_{H_2O} \tag{14}$$

$$0 = S^{l}_{m}\,dT - V^{l}_{m}\,dp + x^{l}_{H_2O}\,d\mu^{l}_{H_2O} + x^{l}_{NaCl}\,d\mu^{l}_{NaCl} \tag{15}$$

$$0 = S^{*s}_{m,H_2O}\,dT - V^{*s}_{m,H_2O}\,dp^s + d\mu^{*s}_{H_2O}. \tag{16}$$

For a simple NaCl aqueous solution, $x^{l}_{NaCl} = 1 - x^{l}_{H_2O}$, the following relation is derived by steps similar to those that led to eq 9:

$$\left(\frac{S^{*s}_{m,H_2O} - S^{*g}_{m,H_2O}}{V^{*s}_{m,H_2O} - V^{*g}_{m,H_2O}} - \frac{S^{l}_{m} - x^{l}_{H_2O}S^{*s}_{m,H_2O}}{V^{l}_{m} - x^{l}_{H_2O}V^{*s}_{m,H_2O}}\right)dT$$

$$= \frac{V^{*g}_{m,H_2O}}{V^{*g}_{m,H_2O} - V^{*s}_{m,H_2O}}\;d\left(\gamma^{sg}\frac{dA^{sg}_{s,m}}{dV^{g}_{m}}\right) - \frac{V^{l}_{m}}{V^{l}_{m} - x^{l}_{H_2O}V^{*s}_{m,H_2O}}\;d\left(\gamma^{ls}\frac{dA^{ls}_{s,m}}{dV^{l}_{m}}\right)$$

$$+ \frac{x^{l}_{NaCl}}{V^{l}_{m} - x^{l}_{H_2O}V^{*s}_{m,H_2O}}\;d\mu^{l}_{NaCl}. \tag{17}$$

As before, by noting that $V^{*g}_{m,H_2O} >> V^{l}_{m,H_2O}$ and by assuming that $\gamma^{sg}\frac{dA^{sg}_{s,m}}{dV^{g}_{m}} = 0$, the following relation is obtained:

$$\left(S^{l}_{m} - x^{l}_{H_2O}S^{*s}_{m,H_2O}\right)dT = V^{l}_{m}\,d\left(\gamma^{ls}\frac{dA^{ls}_{s,m}}{dV^{l}_{m}}\right) - x^{l}_{NaCl}\,d\mu^{l}_{NaCl} \tag{18}$$

which yields on rearrangement

$$V^{l}_{m}\,d\left(\gamma^{ls}\frac{dA^{ls}_{s,m}}{dV^{l}_{m}}\right) = \left(S^{l}_{m} - x^{l}_{H_2O}S^{*s}_{m,H_2O} + x^{l}_{NaCl}\frac{d\mu^{l}_{NaCl}}{dT}\right)dT\,. \tag{19}$$

The ice-solution capillary pressure can be calculated as a function of temperature with

$$p_c = \int_{T_0}^{T} \frac{S^{l}_{m} - x^{l}_{H_2O}S^{*s}_{m,H_2O} + x^{l}_{NaCl}\frac{d\mu^{l}_{NaCl}}{dT}}{V^{l}_{m}}\;dT. \tag{20}$$

To calculate ice-solution capillary pressure, the quantities in the integrand must be calculated. These quantities are

1. The mole fractions of the solute and solvent
2. The melting point of the solution phase in bulk
3. The molar entropy of ice
4. The molar entropy of the liquid solution
5. The molar volume of the liquid solution
6. The temperature derivative of the solute chemical potential.

Relationship of capillary pressures to pore radii and liquid-water contents

Defay and Prigogine (1966) have derived a form of the Laplace equation for freezing liquids in saturated porous media:

$$p_c = -\frac{2\gamma^{ls}}{r^{ls}} \tag{21}$$

where r^{ls} is the radius of a concave liquid/solid interface in a pore. Brun et al. (1977) found that r^{ls} is equal to the pore radius less the few molecular diameters corresponding to the liquid that wets the pore solid surfaces, which remains unfrozen to temperatures well below the bulk melting point. Experimentally measured freezing curves of porous solids are consistent with a general relationship between liquid/solid capillary pressure and the specific volume of unfrozen liquid. For a given capillary pressure corresponding to a particular pore radius, it is assumed generally that the contents of all narrower pores are unfrozen and the contents of all wider pores are solidified. This capillary pressure–unfrozen liquid relationship is physical and should be unaffected directly by the chemical composition of the phases. For a given porous material, therefore, it is expected that this relationship will be general and unaffected by phase composition. We tested this expectation with experiments described in the following section.

MATERIALS AND METHODS

Sample preparation

Kaolinite clay

Approximately 40 g of clay were washed five times with 200 mL of 1-mol kg^{-1} NaCl aqueous solution to saturate the cation exchange complex with Na^+. In each washing, the clay–solution suspension was stirred for about 5–15 minutes with a vortex stirrer. The solids were separated with a centrifuge.

Following the last washing with 1-mol kg^{-1} NaCl solution, the suspension was separated into three aliquots and individually washed with 0.1-, 0.01-, and 0.001-mol kg^{-1} NaCl solutions, respectively. These washings were followed by centrifugation; this process was repeated four times. The individual samples were then sealed in test tubes with rubber stoppers to prevent moisture changes.

Montmorillonite clay

Sodium-saturated montmorillonite that had been prepared previously for other experiments and then stored was selected for analysis. Three 4-g samples of this clay were placed in beakers to which 200-mL solutions of either 0.1-, 0.01-, or 0.001-mol kg^{-1} NaCl were added. The clays were then separated from the solutions and resuspended five times with further washings of 200-mL solutions of 0.1-, 0.01-, and 0.001-mol kg^{-1} NaCl. The 0.1-mol kg^{-1} suspension was centrifuged at high speed for approximately 6 hours. The liquids in the 0.01- and 0.001-mol kg^{-1} suspensions were separated from the clay by pressure-membrane extraction. Following the above treatments, the samples were placed in sealed test tubes.

Quartz sand

A fine-textured sand was divided into three 50-g subsamples that were washed four times with either 0.1-, 0.01-, or 0.001-mol kg^{-1} NaCl solution. Each saturated sand sample was sealed in test tubes.

Experimental procedure

Once the mineral pastes were placed in their respective test tubes, at least two days were allowed for moisture equilibration before the unfrozen water content was determined. Following this period, the sealed tubes containing minerals and solutions were placed in a bath preset to an initial test temperature of about 20°C. If the analysis temperatures were within the range of 20°C to –20°C, the bath heat-transfer fluid was an ethylene glycol–water mixture. If the analysis required temperatures below –20°C, a second bath that used methyl alcohol as a heat-transfer fluid and was capable of achieving temperatures of –70°C was utilized.

Following a temperature equilibration time of approximately 1 hour, the sample tubes were sequentially removed from the bath, wiped dry, and inserted into the nuclear magnetic resonance (NMR) probe for analysis. (The mean background signal intensity due to the test tube was measured by placing an empty test tube in the NMR probe.) The peak intensity for each temperature was recorded. The NMR probe used for these analyses was a Praxis model PR-103 analyzer. It was operated in the 90° mode with a 0.2-s clock and at a fast scan speed. The first pulse amplitude in the 90° mode was measured for each sample, starting with the first test temperature of about 20°C. After about 4 s (the time required to measure the NMR signal amplitude) the samples were reinserted into the bath. When all the samples were analyzed, the bath temperature was lowered by about 3°C and allowed to re-equilibrate at this new test temperature. This process was repeated until a temperature of about 0°C was reached. (All of the above-0°C NMR measurements were used to determine the paramagnetic effect or the increase in signal intensity with decreasing temperature. This relationship is discussed by Tice et al. [1981, 1982].)

Once measurements above 0°C were completed, the constant-temperature bath was cooled to about –5°C to initiate ice formation in the samples. The constant-temperature bath was then raised to –0.5°C, and the samples were allowed to equilibrate at this temperature for several hours. After equilibration, the peak intensity and temperature were recorded. The temperature of the constant-temperature bath was then lowered in small increments. The signal intensity and temperature were recorded after the sample was allowed to equilibrate at each temperature increment. The samples were cooled until the measured signal intensity matched that for an empty test tube—indicating that no liquid water remained in the sample (Tice 1982).

Following the last NMR cooling measurements, which in some instances were taken at temperatures as cold as –77°C, the warming run was begun. An analysis interval of about 4°C was selected at the lower temperatures, at which small changes in temperature have little effect on signal intensity. At temperatures near melting, intervals between equilibration temperatures were reduced because liquid-water contents were increasing more with temperature. At around –1°C, the interval by which the temperature was changed was reduced to about –0.1°C. This approach provided good coverage within the region where the unfrozen water–temperature relationship is so critical.

Unfrozen water contents were calculated by first regressing the above-0°C NMR readings minus the background against their respective temperatures for each sample and extending the resultant line to the lowest temperature where experimental data were obtained. Projected first-pulse amplitudes were calculated for each experimental temperature. The gravimetric water content for each sample had previously been determined by oven-drying at 110°C for two days. A ratio between the sample water content and the projected first-pulse amplitude was developed; unfrozen water contents were calculated by multiplying these first-pulse amplitudes by their respective ratios to obtain a value for each temperature (Tice et al. 1981, 1982).

EXPERIMENTAL RESULTS

The mean initial specific water contents and equilibrating-solution molalities for the pastes are presented in Table 1. The specific liquid water contents of the pastes as measured by pulsed NMR are presented in Tables 2 through 7, and their liquid water contents are presented graphically in Figures 1 through 6.

For a given initial solution molality, the freezing curves of all pastes displayed the roughly exponential decline in liquid-water content with decreasing temperature that is characteristic of freezing curves. The freezing curves of the sand pastes were much less smooth than those for the kaolinite or montmorillonite pastes because of the much lower intensity of the peak signal from the sand samples. There was no pronounced hysteresis between the cooling and heating curves for any of the samples. For each of the three minerals, the freezing curves of the pastes that had been equilibrated with 0.001-mol kg^{-1} NaCl solutions were roughly coincident with those that were equilibrated with 0.01-mol kg^{-1} NaCl solutions. For each mineral, the freezing curves of the pastes initially equilibrated with 0.1-mol kg^{-1} NaCl solutions showed more liquid water at a given temperature than those equilibrated with the lower-molality solutions. This shifting in the curves was likely the result of the depression of the freezing points of the higher-molality solution. On a relative basis, this shift was most pronounced for the sand samples and least pronounced for the kaolinite samples.

COMPARISON WITH THEORY

In this section we first detail how the capillary pressures and specific volumes of the pore water solutions were calculated. These calculated values are then presented graphically and analyzed.

Calculation of the necessary thermophysical properties

As stated earlier, the following thermodynamic quantities are needed to calculate ice-solution capillary pressures in frozen porous media:

1. The mole fractions of the solute and solvent
2. The freezing point of the solution phase in bulk
3. The molar entropy of ice
4. The molar entropy of the liquid solution
5. The molar volume of the liquid solution
6. The temperature derivative of the solute chemical potential.

Table 1. Equilibrating solution molalities and total specific water masses for pastes frozen then thawed in this study.

Mineral	*Initial NaCl molality (mol kg^{-1})*	*Initial specific water content (kg kg^{-1})*
Kaolinite	0.100 471	2.3425
	0.010 031 4	2.6703
	0.001 002 98	2.1865
Montmorillonite	0.100 471	35.8610
	0.010 031 4	31.5064
	0.001 002 98	12.5529
Sand	0.100 471	0.2165
	0.010 031 4	0.2146
	0.001 002 98	0.2225

Mole fractions of the solute and solvent

A bulk H_2O–NaCl system under atmospheric pressure has a precisely defined eutectic point at 252 K (–21.15°C) and 5.14 mol kg^{-1}. Below the eutectic temperature no liquid phase remains, giving way to a mixed solid phase composed of hexagonal ice [rep-

Table 2. Unfrozen-water contents, as measured by pulsed NMR, of kaolinite pastes cooled from 0°C to –66.6°C.

	Specific liquid water content (kg kg^{-1})		
	Initial NaCl solution molality		
Temperature (°C)	*0.1 mol kg^{-1}*	*0.01 mol kg^{-1}*	*0.001 mol kg^{-1}*
–0.25		0.9873	0.7821
–0.34		0.8281	0.6542
–0.43		0.6231	0.5024
–0.52	1.6059	0.5011	0.4332
–0.61	1.5677	0.4769	0.4255
–0.76	1.3924	0.4361	0.3982
–0.81	1.2570	0.4267	0.3817
–0.89	1.1216	0.4026	0.3755
–1.10	0.8735	0.3838	0.3721
–1.20	0.8146	0.3780	0.3480
–1.29	0.7493	0.3650	0.3419
–1.45	0.6774	0.3482	0.3371
–1.54	0.6333	0.3498	0.3325
–1.76	0.5856	0.3439	0.3083
–1.96	0.5284	0.3124	0.2737
–2.15	0.4875	0.2719	0.2437
–2.43	0.4562	0.2478	0.2211
–2.69	0.4233	0.2111	0.1986
–3.02	0.4017	0.1998	0.1790
–3.21	0.3868	0.1723	0.1537
–3.75	0.3553	0.1501	0.1371
–4.40	0.3046	0.1135	0.1072
–5.70	0.2328	0.0841	0.0803
–7.20	0.1917	0.0656	0.0579
–9.00	0.1416	0.0474	0.0431
–11.00	0.1063	0.0347	0.0327
–14.10	0.0773	0.0273	0.0238
–17.00	0.0598	0.0219	0.0207
–20.00	0.0515	0.0165	0.0163
–23.00	0.0421	0.0130	0.0107
–24.70	0.0432	0.0145	0.0120
–26.70	0.0356	0.0080	0.0092
–28.80	0.0324	0.0079	0.0117
–30.60	0.0308	0.0063	0.0104
–33.80	0.0276	0.0077	0.0089
–39.00	0.0188	0.0075	0.0062
–45.20	0.0052	0.0044	0.0024
–49.80	0.0038		0.0048
–55.30	0.0025		0.0047

Note: The equilibrating solutions of the pastes were initially 0.1, 0.01, and 0.001 mol kg^{-1} NaCl. Data are not presented for temperatures at which no liquid water was detected.

Table 3. Unfrozen-water contents, as measured by pulsed NMR, of kaolinite pastes warmed from –66.6°C to 0°C.

	Specific liquid water content (kg kg^{-1})		
	Initial NaCl solution molality		
Temperature (°C)	*0.1 mol kg^{-1}*	*0.01 mol kg^{-1}*	*0.001 mol kg^{-1}*
–61.20	0.0024		0.0023
–55.60	0.0013	0.0028	0.0012
–50.10	0.0038	0.0029	0.0036
–44.80	0.0052	0.0073	0.0061
–39.30	0.0081	0.0090	0.0087
–34.60	0.0096	0.0092	0.0114
–30.60	0.0182	0.0078	0.0117
–28.20	0.0212	0.0127	0.0157
–26.40	0.0314	0.0144	0.0132
–24.50	0.0389	0.0129	0.0160
–22.40	0.0436	0.0131	0.0121
–19.20	0.0532	0.0183	0.0177
–17.30	0.0597	0.0235	0.0193
–13.60	0.0790	0.0257	0.0224
–10.40	0.1051	0.0383	0.0342
–7.90	0.1534	0.0530	0.0519
–6.00	0.1992	0.0732	0.0627
–4.20	0.2874	0.1064	0.0926
–3.26	0.3578	0.1578	0.1389
–2.80	0.3877	0.1782	0.1644
–2.18	0.4649	0.2391	0.2006
–1.75	0.5226	0.2781	0.2517
–1.63	0.5537	0.3149	0.2787
–1.50	0.5767	0.3316	0.2863
–1.33	0.6113	0.3558	0.3209
–1.20	0.6377	0.3670	0.3316
–1.13	0.6672	0.3764	0.3511
–1.01	0.6855	0.3895	0.3618
–0.97	0.7003	0.3657	0.3499
–0.86	0.7332	0.3806	0.3501
–0.80	0.7708	0.4010	0.3637
–0.65	0.8040	0.4142	0.3715
–0.58	0.8353	0.4384	0.3896
–0.50	0.8780	0.5012	0.4123
–0.34	0.9293	0.5939	0.4876
–0.27	0.9851	0.6532	0.5448
–0.21		0.7365	0.6186
–0.19		0.7642	0.6502
–0.14		0.8217	0.6999
–0.08		0.8737	0.7467
–0.02		0.9498	0.8056

Note: The equilibrating solutions of the pastes were initially 0.1, 0.01, and 0.001 mol kg^{-1} NaCl. Data are not presented for temperatures at which no liquid water was detected.

Table 4. Unfrozen-water contents, as measured by pulsed NMR, of montmorillonite pastes cooled from 0°C to –66.6°C.

	Specific liquid water content (kg kg^{-1})		
	Initial NaCl solution molality		
Temperature (°C)	*0.1 mol kg^{-1}*	*0.01 mol kg^{-1}*	*0.001 mol kg^{-1}*
–0.14		2.5987	1.8358
–0.25		1.9654	1.5490
–0.34		1.6137	1.1300
–0.43		1.2097	0.8856
–0.52		1.1391	0.6413
–0.61		0.8583	0.5854
–0.76		0.7351	0.5433
–0.81		0.7174	0.5292
–0.89		0.6647	0.4316
–1.10		0.6465	0.4313
–1.20		0.5938	0.3964
–1.29		0.7332	0.3823
–1.45		0.6453	0.3752
–1.54		0.6974	0.3889
–1.76		0.6617	0.3748
–1.96		0.6089	0.3606
–2.15		0.5735	0.3188
–2.43	16.0658	0.5207	0.3254
–2.69	5.3741	0.5200	0.3251
–3.02	4.6635	0.5018	0.3040
–3.21	4.2586	0.4840	0.2969
–3.75	3.8469	0.4655	0.2757
–4.40	3.3165	0.3952	0.2682
–5.70	2.6221	0.3244	0.2259
–7.20	2.0724	0.2712	0.1906
–9.00	1.5292	0.1848	0.1489
–11.00	1.1680	0.1497	0.1277
–14.10	0.8850	0.1147	0.1130
–17.00	0.7046	0.1132	0.1054
–20.00	0.5659	0.0797	0.1043
–23.00	0.4494	0.0472	0.1033
–24.70	0.4277	0.0624	0.0834
–26.70	0.4058	0.0773	0.0765
–28.80		0.0613	0.0760
–30.60			0.0693
–33.80			0.0623
–39.00			0.0490
–45.20			0.0541
–49.80			0.0297
–55.30			0.0175
–60.70			0.0230
–61.20			
–66.60			

Note: The equilibrating solutions of the pastes were initially 0.1, 0.01, and 0.001 mol kg^{-1} NaCl. Data are not presented for temperatures at which no liquid water was detected.

Table 5. Unfrozen-water contents, as measured by pulsed NMR, of montmorillonite pastes warmed from –66.6°C to 0°C.

	Specific liquid water content (kg kg^{-1})		
	Initial NaCl solution molality		
Temperature (°C)	*0.1 mol kg^{-1}*	*0.01 mol kg^{-1}*	*0.001 mol kg^{-1}*
–61.20	0.0000	0.0000	0.0000
–55.60	0.0000	0.0000	0.0350
–50.10	0.0000	0.0000	0.0415
–44.80	0.0000	0.0000	0.0361
–39.30	0.0332	0.0293	0.0613
–34.60	0.0509	0.0448	0.0559
–30.60	0.0519	0.0760	0.0756
–28.20	0.1051	0.0768	0.0825
–26.40	0.0883	0.0619	0.0830
–24.50	0.1249	0.0937	0.0963
–22.40	0.1262	0.0788	0.0970
–19.20	0.5682	0.0800	0.1046
–17.30	0.6109	0.0807	0.1052
–13.60	0.8118	0.1150	0.1132
–10.40	1.1910	0.1668	0.1347
–7.90	1.7528	0.2533	0.1494
–6.00	2.1847	0.2898	0.1573
–4.20	3.0220	0.4300	0.1858
–3.26	3.8376	0.5185	0.2761
–2.80	4.1884	0.6410	0.2904
–2.18	5.1082	0.6603	0.3188
–1.75	6.1489	0.7314	0.3609
–1.63	7.0005	0.7145	0.3819
–1.50	7.4095	0.7498	0.3959
–1.33	8.6090	0.8377	0.3753
–1.20	10.1929	0.9081	0.3825
–1.13	11.4315	0.9434	0.3895
–1.01	12.4109	0.9090	0.4384
–0.97	12.9605	1.0665	0.4385
–0.86	14.0224	1.1021	0.4804
–0.80	15.2435	0.9450	0.5084
–0.65	16.8189	1.0333	0.5783
–0.58	18.4088	1.2439	0.5854
–0.50	20.1838	1.3320	0.6762
–0.34	22.5804	1.7716	0.9068
–0.27	25.3344	2.0179	1.1093
–0.21	0.0000	1.9659	1.3189
–0.19	0.0000	2.1240	1.4307
–0.14	0.0000	2.7216	1.7939
–0.08	0.0000	3.4426	2.1993
–0.02	0.0000	4.4276	2.7235

Note: The equilibrating solutions of the pastes were initially 0.1, 0.01, and 0.001 mol kg^{-1} NaCl. Data are not presented for temperatures at which no liquid water was detected.

Table 6. Unfrozen-water contents, as measured by pulsed NMR, of sand pastes cooled from 0°C to –66.6°C.

	Specific liquid water content (kg kg⁻¹)		
	Initial NaCl solution molality		
Temperature (°C)	*0.1 mol kg⁻¹*	*0.01 mol kg⁻¹*	*0.001 mol kg⁻¹*
–0.14		0.0145	0.0119
–0.25		0.0106	0.0069
–0.34		0.0096	0.0040
–0.43		0.0096	
–0.52		0.0086	
–0.61		0.0067	
–0.76		0.0067	
–0.81		0.0038	
–0.89		0.0048	
–1.10		0.0076	
–1.20		0.0067	
–1.29		0.0057	
–1.45		0.0047	
–1.54		0.0085	
–1.76		0.0085	
–1.96		0.0066	
–2.15	0.0481	0.0066	
–2.43	0.0461	0.0066	
–2.69	0.0431	0.0056	
–3.02	0.0392	0.0047	
–3.21	0.0410	0.0056	
–3.75	0.0380	0.0046	
–4.40	0.0340	0.0046	
–5.70	0.0290	0.0045	
–7.20	0.0214		
–9.00	0.0149		
–11.00	0.0111		
–14.10	0.0075		
–17.00	0.0056		
–20.00	0.0039		
–23.00	0.0023		
–24.70	0.0023		

Note: The equilibrating solutions of the pastes were initially 0.1, 0.01, and 0.001 mol kg^{-1} NaCl. Data are not presented for temperatures at which no liquid water was detected.

Table 7. Unfrozen-water contents, as measured by pulsed NMR, of sand pastes warmed from –66.6°C to 0°C.

	Specific liquid water content (kg kg⁻¹)		
	Initial NaCl solution molality		
Temperature (°C)	*0.1 mol kg⁻¹*	*0.01 mol kg⁻¹*	*0.001 mol kg⁻¹*
–19.20	0.0039		
–17.30	0.0056		
–13.60	0.0083		
–10.40	0.0147	0.0026	
–7.90	0.0257	0.0062	
–6.00	0.0298	0.0045	
–4.20	0.0387	0.0065	
–3.26	0.0559	0.0102	
–2.80	0.0571	0.0122	
–2.18	0.0669	0.0132	
–1.75	0.0796	0.0133	
–1.63	0.0787	0.0133	
–1.50	0.0817	0.0123	
–1.33	0.0828	0.0124	
–1.20	0.0877	0.0124	
–1.13	0.0992	0.0133	
–1.01	0.1041	0.0115	
–0.97	0.1032	0.0115	
–0.86	0.1148	0.0115	
–0.80	0.1207	0.0086	
–0.65	0.1372	0.0125	
–0.58	0.1488	0.0134	
–0.50	0.1634	0.0144	
–0.34	0.1897	0.0173	
–0.27	0.2062	0.0154	
–0.21		0.0144	
–0.19		0.0144	0.0089
–0.14		0.0154	0.0099
–0.08		0.0154	0.0139
–0.02		0.0280	0.0199

Note: The equilibrating solutions of the pastes were initially 0.1, 0.01, and 0.001 mol kg^{-1} NaCl. Data are not presented for temperatures at which no liquid water was detected.

resented by H_2O(cr,I)] and hydrohalite, $NaCl \cdot 2H_2O$(cr) (Archer 1992). Our calculations of solution molalities assumed implicitly that all of the NaCl remained in solution as ice was formed. We did not calculate the molalities of solutions for observations below 252 K, since the possible formation of hydrohalite at these temperatures invalidated our assumption that all of the NaCl remained in the liquid phase. The molality of the liquid solution at a particular temperature of interest T_f was calculated by

$$m_{T_f} = \frac{m_i \theta_i}{\theta_{T_f}} \tag{22}$$

where m_i = initial NaCl molality of solutions of pastes (mol kg^{-1})
m_{T_f} = NaCl molality of solutions of pastes at temperature T_f (mol kg^{-1})
θ_i = initial specific liquid-water content (kg kg^{-1})
θ_{T_f} = specific liquid-water content at $T = T_f$ (kg kg^{-1}).

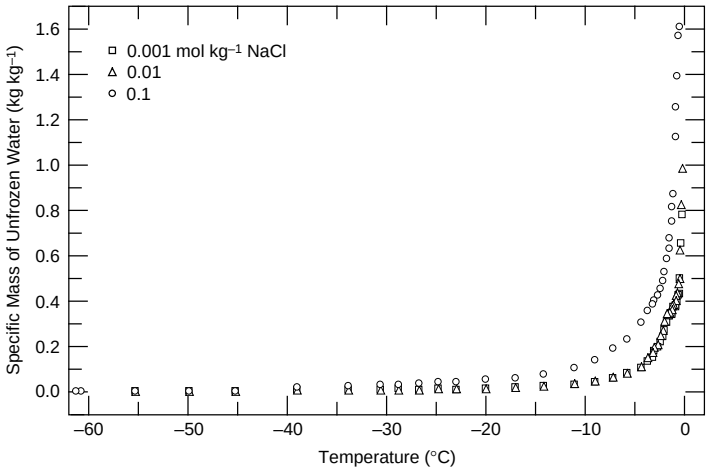

Figure 1. Unfrozen water contents, as measured by pulsed NMR, of freezing kaolinite pastes cooled from 0°C to –66.6°C. The equilibrating solutions of the pastes were initially 0.1, 0.01, and 0.001 mol kg^{-1} NaCl.

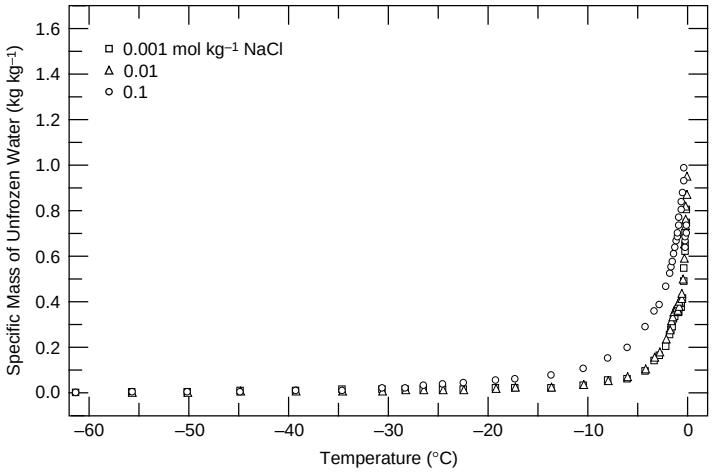

Figure 2. Unfrozen water contents, as measured by pulsed NMR, of freezing kaolinite pastes warmed from –66.6°C to 0°C. The equilibrating solutions of the pastes were initially 0.1, 0.01, and 0.001 mol kg^{-1} NaCl.

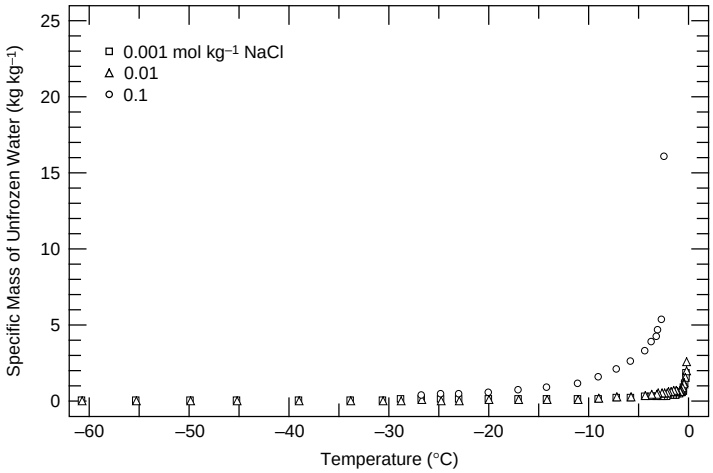

Figure 3. Unfrozen water contents, as measured by pulsed NMR, of freezing montmorillonite pastes cooled from 0°C to –66.6°C. The equilibrating solutions of the pastes were initially 0.1, 0.01, and 0.001 mol kg^{-1} NaCl.

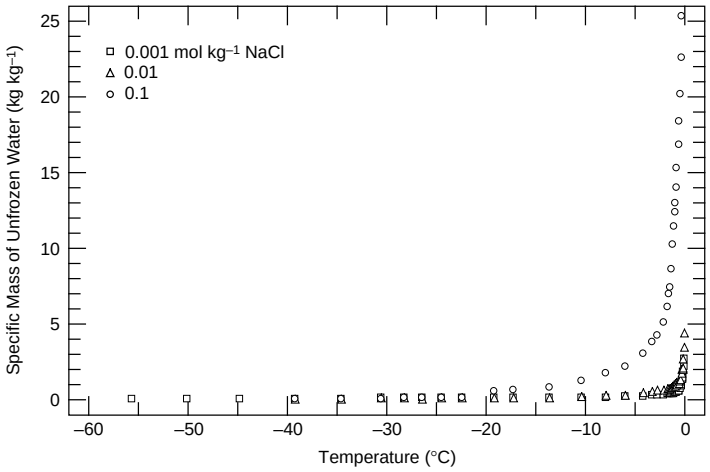

Figure 4. Unfrozen water contents, as measured by pulsed NMR, of freezing montmorillonite pastes warmed from –66.6°C to 0°C. The equilibrating solutions of the pastes were initially 0.1, 0.01, and 0.001 mol kg^{-1} NaCl.

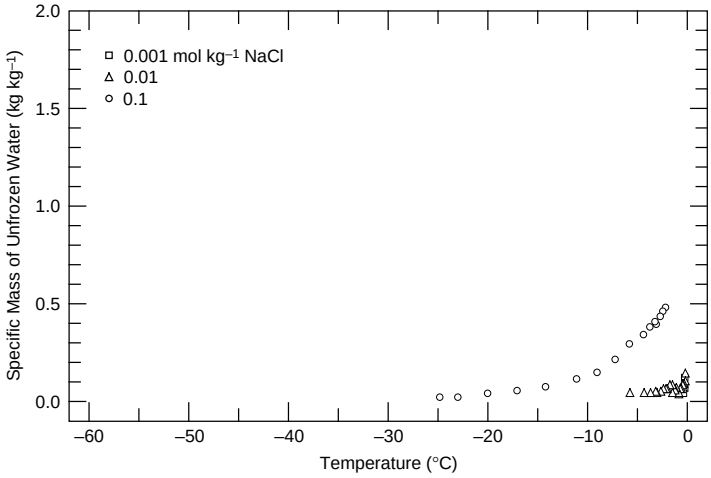

Figure 5. Unfrozen water contents, as measured by pulsed NMR, of freezing sand pastes cooled from 0°C to –66.6°C. The equilibrating solutions of the pastes were initially 0.1, 0.01, and 0.001 mol kg^{-1} NaCl.

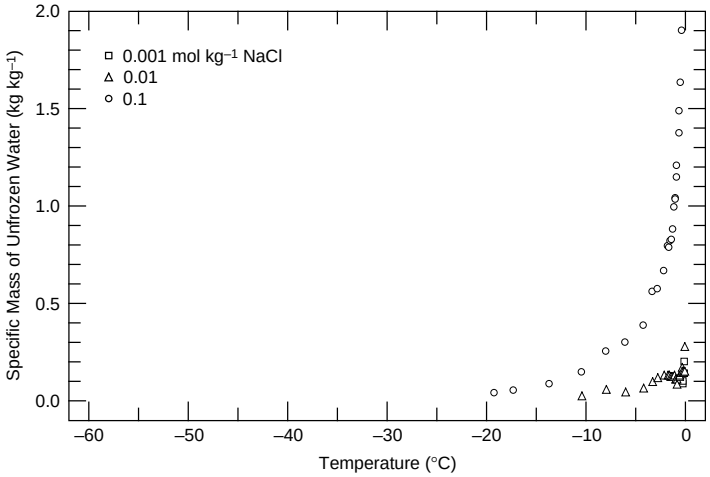

Figure 6. Unfrozen water contents, as measured by pulsed NMR, of freezing sand pastes warmed from –66.6°C to 0°C. The equilibrating solutions of the pastes were initially 0.1, 0.01, and 0.001 mol kg^{-1} NaCl.

The solvent and solute mole fractions could be calculated by:

$$x_{\mathrm{NaCl}} = \frac{m_{T_\mathrm{f}}}{m_{T_\mathrm{f}} + \frac{1}{M_{\mathrm{H_2O}}}} \tag{23}$$

$$x_{\mathrm{H_2O}} = 1 - x_{\mathrm{NaCl}} \tag{24}$$

where $M_{\mathrm{H_2O}}$ is the molar mass of water (0.018 015 28 kg mol^{-1}).

Freezing point of the solution phase in bulk

We fitted by regression the freezing-point depression data calculated by the Fortran program FREZCHEM (Marion and Grant 1994) for the H_2O–NaCl expression:

$$T_0 = 273.15 - K_f m_{\mathrm{NaCl\,(aq)}} \tag{25}$$

where K_f is an approximate cryoscopic constant for the H_2O–NaCl system, which we found to be 4.12207 K kg mol^{-1}. This compares with the expected cryoscopic constant for a single electrolyte completely disassociated in water of 3.72 K kg mol^{-1} (Atkins 1990).

Molar entropy of ice

The quantity $S^{*\mathrm{s}}_{\mathrm{m},\mathrm{H_2O}} \equiv S^*_\mathrm{m}\left[\mathrm{H_2O(cr,I)}\right]$ at a temperature and pressure of interest can be calculated by adding the entropy changes due to cooling and freezing to the entropy of water at a reference point (i.e., T_r = 273.15 K and p_r = 0.1 MPa). This quantity is calculated by evaluating

$$S^*_{\mathrm{m},p_r}\left[\mathrm{H_2O(cr,I)}\right] = S^*_{\mathrm{m},T_r,p_r}\left[\mathrm{H_2O(l)}\right] \tag{26}$$

$$+ \quad \Delta^{T=273.15}_{T_r} S^*_\mathrm{m}\left[\mathrm{H_2O(l)}, p_r\right] \tag{27}$$

$$+ \quad \Delta^{\mathrm{l}}_{\mathrm{cr,I}} S^*_\mathrm{m}\left(\mathrm{H_2O}, T = 273.15, p_r\right) \tag{28}$$

$$+ \quad \Delta^{T=273.15}_{T_\mathrm{f}} S^*_\mathrm{m}\left[\mathrm{H_2O(cr,I)}, p_r\right]. \tag{29}$$

The starting point of the calculation (eq 26) is the molar entropy of pure water at a reference temperature (T_r = 273.15 K) and pressure (p_r = 0.1 MPa), for which the standard-state molar entropy, $S^*_{\mathrm{m},T_r,p_r}\left[\mathrm{H_2O(l)}\right]$, is 69.950 J K^{-1} mol^{-1} (Chase et al. 1985).

Haida et al. (1974) reported the entropy change due to the constant-pressure cooling of water from 298.15 K to its freezing point, $\Delta^{T=273.15}_{T_r} S^*_\mathrm{m}\left[\mathrm{H_2O(l)}, p_r\right]$ = 6.615 ± 0.01 (eq 27). This quantity can also be calculated with the equation-of-state model for water (Hill 1990):

$$S^*_{\mathrm{H_2O(l)}}\left(T_{rw}, p_{rc}\right) - S^*_{\mathrm{H_2O(l)}}\left(T_{rc}, p_{rc}\right) = -6.616\ 04\ \ \mathrm{J\,K^{-1}\ mol^{-1}} \tag{30}$$

We used the latter value in our calculations.

The entropy change associated with freezing (eq 28), $\Delta^{\mathrm{l}}_{\mathrm{cr,I}} S^*_\mathrm{m}\left(\mathrm{H_2O}, T = 273.15, p_r\right)$ is calculated by

$$\Delta^{\mathrm{l}}_{\mathrm{cr,I}} S^*_\mathrm{m}\left(\mathrm{H_2O}, T = 273.15, p_r\right) = \frac{\Delta^{\mathrm{l}}_{\mathrm{cr,I}} H^*_\mathrm{m}\left(\mathrm{H_2O}, T = 273.15, p_r\right)}{273.15}\ . \tag{31}$$

Haida et al. (1974) reported a molar enthalpy of melting of 6006.8 J mol^{-1}. Giauque and Stout (1936) earlier reported a value of 6007.0 ± 3.8 J mol^{-1}.

The constant-pressure entropy change due to changes in temperature of a pure substance (eq 29) is calculated by

$$\Delta_{T_1}^{T_2} S_{\mathrm{m}}^{*} = \int_{T_1}^{T_2} \frac{C_p^{*}}{T}\, \mathrm{d}T \ . \tag{32}$$

As with many solids, the heat capacity of H_2O(cr,I) as a function of temperature can be described by the Maier–Kelly (1932) equation:

$$C_p = a + bT + \frac{c}{T^2}. \tag{33}$$

Values of $C^{*}_{p,\mathrm{H_2O(cr,I)}}$ between T = 198.57 K and 268.39 K reported by Haida et al. (1974) were fitted by nonlinear regression (Marquardt procedure) to eq 33 (SAS Institute 1985). The data of Haida et al. (1974) and the fitted line are presented in Figure 7. The regression had a coefficient of determination (R^2) of 0.999 997. The following parameter estimates (with parameter-estimate standard errors in parentheses) were obtained:

a = –10.6644 (1.5999) J K^{-1} mol^{-1}

b = 0.1698 (0.0046) J K^{-2} mol^{-1}

c = 198 148. (28 230.) J K mol^{-1} .

Equation 32 was calculated by

$$\int_{T_{\mathrm{rw}}}^{T_{\mathrm{f}}} \frac{C^{*}_{p,\mathrm{H_2O(cr,I)}}}{T}\, \mathrm{d}T = a\left[\ln\left(T_{\mathrm{f}}\right) - \ln\left(T_{rw}\right)\right] + b\left(T_{\mathrm{f}} - bT_{rw}\right) + \frac{c}{2\left(T_{rw}^2 - T_{\mathrm{f}}^2\right)}. \tag{34}$$

Molar entropies of electrolyte solutions

The procedure for calculating the molar entropies of electrolyte solutions can be derived from equations found in standard texts on chemical thermodynamics (e.g., p. 152–154 in Lupis [1983]). The entropy of a mixture or solution [S_{M} (J K^{-1})] composed of n_{A} moles of A (by convention, the solvent) and n_{B} moles of B (again, by convention, the solute) is

$$S_{\mathrm{M}} = S_{\mathrm{A}} + S_{\mathrm{B}}. \tag{35}$$

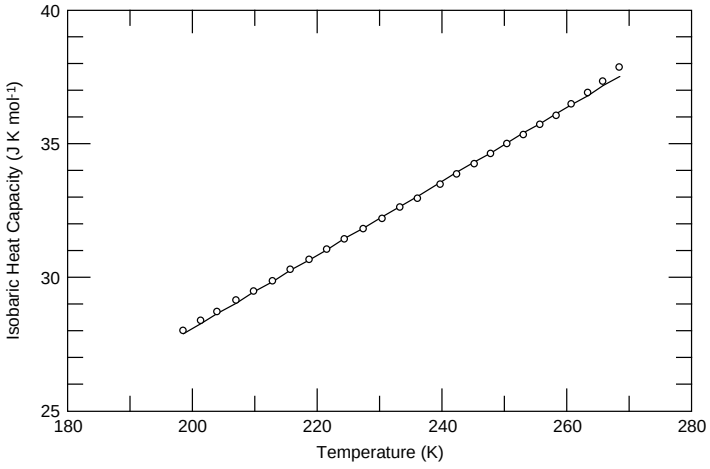

Figure 7. Constant-pressure heat capacity of H_2O(cr,I) under p = *0.101325 MPa and* T = *200 K to 268 K as reported by Haida et al. (1974). The line was calculated by a regression fit of the data to the Maier–Kelly model.*

Defining the total number of moles in the solution as $n_T = n_A + n_B$, this is equivalent to

$$n_T S_{m,M} = n_A S_{m,A} + n_B S_{m,B} \tag{36}$$

where $S_{m,A}$ is the molar entropy of component A (J K^{-1} mol^{-1}) and $S_{m,M}$ is the molar entropy of the mixture, so

$$S_{m,M} \equiv S_m^l = x_A S_{m,A} + x_B S_{m,B}. \tag{37}$$

The calculation of $S_{m,M}$ is facilitated by defining the molar entropy of mixing, $\Delta_{mix}S_{m,M}$, as

$$\Delta_{mix}S_{m,M} = S_{m,M} - x_A S^{\Theta}_{m,A} - x_B S^{\Theta}_{m,B} \tag{38}$$

where $S^{\Theta}_{m,A}$ is the standard-state molar entropy of A. The molar entropy of mixing for the mixture is also equal to the proportional sum of the molar entropies of mixing for all components in the solution:

$$\Delta_{mix}S_{m,M} = x_A \Delta_{mix}S_{m,A} + x_B \Delta_{mix}S_{m,B} \tag{39}$$

where $\Delta_{mix}S_{m,A}$ is the molar entropy of mixing for component A. For each mixture component *i*, the molar entropy of mixing can be calculated by

$$\Delta_{mix}S_{m,i} = -\left[\frac{\partial\left(\Delta_{mix}G_{m,i}\right)}{\partial T}\right]_p = -R\ln a_{x,i} - RT\left(\frac{\partial \ln a_{x,i}}{\partial T}\right)_p \tag{40}$$

where $a_{x,i}$ is the mole-fraction-based activity of component *i*. So that the molar entropy of a solution can be calculated by

$$\begin{aligned} S_{m,M} \equiv S_m^1 \quad = \quad & x_A\left[S^{\Theta}_{m,A} - R\ln a_{x,A} - RT\left(\frac{\partial \ln a_{x,A}}{\partial T}\right)_p\right] \\ + \quad & x_B\left[S^{\Theta}_{m,B} - R\ln a_{x,B} - RT\left(\frac{\partial \ln a_{x,B}}{\partial T}\right)_p\right]. \end{aligned} \tag{41}$$

To evaluate this equation, the following quantities must be determined for the temperatures of interest:

1. The standard-state entropy of the solvent, water
2. The standard-state entropy of the solute, NaCl(aq)
3. The activities of both water and NaCl(aq)
4. The temperature derivatives of the natural logarithms of both activities of the solvent and solute.

Standard-state entropy of liquid water at subzero temperatures. The standard-state entropy of water at subzero temperatures is estimated with the heat capacities of supercooled water.

Speedy (1987) has presented equations for the various thermodynamic proper-

Table 8. Coefficients to Speedy's (1987) empirical equations for calculating the thermophysical properties of supercooled water.

x	$\alpha \times 10^3$ (K)	κ_T (bar^{-1})	C_p ($J\,K^{-1}mol^{-1}$)
C_x	–0.80	20.0	14.2
$B_x^{(0)}$	1.802 180 3	4.120	25.952
$B_x^{(1)}$	–0.941 698 0	–1.130	128.281
$B_x^{(2)}$	0.905 507 0	77.817	14.2
$B_x^{(3)}$	–0.80	–78.143	–221.405
$B_x^{(4)}$		54.290	–64.812
max resid	1.2 ppm	0.2%	0.03%

ties of supercooled water. His expression for the constant-pressure heat capacity of supercooled water is

$$C_p = \sum_{n=0}^{4} B_{C_p}^{(n)} \varepsilon^n + 2C_{C_p} \varepsilon^{-1/2} \tag{42}$$

where $B_{C_p}^{(0)}, \ldots, B_{C_p}^{(4)}$ and C_{C_p} are fitted coefficients. The estimated values of these coefficients are presented in Table 8. The parameter ε is a reduced temperature $\left(= \dfrac{T - T_s}{T_s}\right)$, T_s being a limiting temperature that is assumed to be exactly 227.15 K (–46°C). Figure 8 presents the constant-pressure heat capacity of water as calculated by the models of Hill (1990) and Speedy (1987).

The entropy changes of supercooled water can be calculated by evaluating the integral:

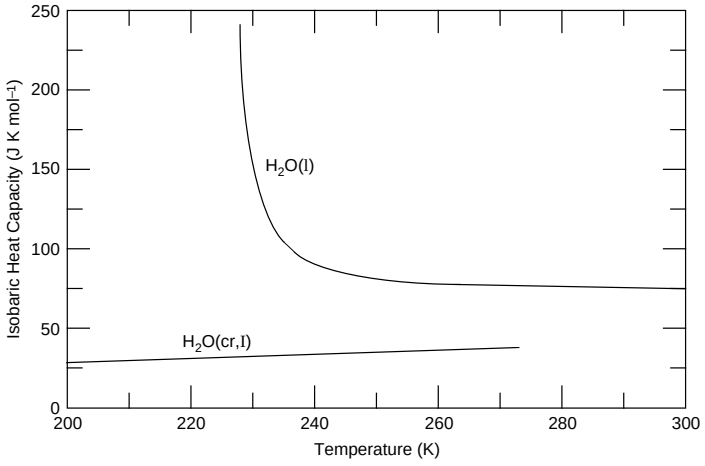

Figure 8. Constant-pressure heat capacity of $H_2O(l)$ and $H_2O(cr,I)$ under p *= 0.101325 MPa and* T *= 200 K to 300 K. $C_p[H_2O(cr,I)]$ values were calculated with the Maier–Kelly model. $C_p[H_2O(l)]$ values between* T *= 200 K and 273 K were calculated with Speedy's (1987) model. $C_p[H_2O(l)]$ values between* T *= 274 K and 300 K were calculated with Hill's (1990) equation-of-state model.*

$$\int_{T_{\mathrm{rw}}}^{T_{\mathrm{f}}} \frac{C^{*}_{p,\mathrm{H_2O(l)}}}{T}\,\mathrm{d}T = \frac{B^{(4)}_{C_p}\left(T_{\mathrm{f}}{}^4 - T_{rw}{}^4\right)}{4T_s^4}$$
$$+ \frac{\left[B^{(3)}_{C_p} - 4B^{(4)}_{C_p}\right]\left(T_{\mathrm{f}}{}^3 - T_{rw}{}^3\right)}{3T_s^3}$$
$$+ \frac{\left[B^{(2)}_{C_p} - 3B^{(3)}_{C_p} + 6B^{(4)}_{C_p}\right]\left(T_{\mathrm{f}}{}^2 - T_{rw}{}^2\right)}{2T_s^2}$$
$$+ \frac{\left[B^{(1)}_{C_p} - 2B^{(2)}_{C_p} + 3B^{(3)}_{C_p} - 4B^{(4)}_{C_p}\right]\left(T_{\mathrm{f}} - T_{rw}\right)}{\mathrm{T}_s}$$
$$+ 2C_{C_p}\arctan\left(\sqrt{\frac{T_{\mathrm{f}}}{T_{\mathrm{s}}} - 1}\right)$$
$$- 2C_{C_p}\arctan\left(\sqrt{\frac{T_{rw}}{T_{\mathrm{s}}} - 1}\right)$$
$$+ \left[B^{(0)}_{C_p} - B^{(1)}_{C_p} + B^{(2)}_{C_p} - B^{(3)}_{C_p} + B^{(4)}_{C_p}\right] \times \left[\ln\left(T_{\mathrm{f}}\right) - \ln\left(T_{rw}\right)\right]. \qquad (43)$$

Standard-state entropy of NaCl(aq). The standard-state entropy of NaCl(aq) is calculated similarly. Initially, we can define the apparent molal constant pressure heat capacity of the solute, ${}^{\phi}C_{p,\mathrm{NaCl(aq)}}$ (J K^{-1} mol^{-1}), in a NaCl aqueous solution as

$${}^{\phi}C_{p,\mathrm{NaCl(aq)}} = \frac{\left[C_{p,\mathrm{m}} - n_{\mathrm{H_2O(l)}}C^{\Theta}_{p,\mathrm{H_2O(l)}}\right]}{n_{\mathrm{NaCl(aq)}}} \qquad (44)$$

where $C_{p,\mathrm{m}}$ = constant-pressure molar heat capacity of the solution (J K^{-1} mol^{-1})
$C^{\Theta}_{p,\mathrm{H_2O(l)}}$ = constant-pressure heat capacity of liquid water in its standard state (i.e., pure) (J K^{-1} mol^{-1})
$n_{\mathrm{H_2O(l)}}$ = amount of water in the solution (mol)
$n_{\mathrm{NaCl(aq)}}$ = amount of NaCl in the solution (mol).

The change in entropy for the solute in its reference state is calculated from

$$\Delta S^{\Theta}_{\mathrm{NaCl(aq)}} = \int_{T_r}^{T} \frac{{}^{\phi}C^{\Theta}_{p,\mathrm{NaCl(aq)}}}{T}\,\mathrm{d}T\ . \qquad (45)$$

The apparent molal constant-pressure heat capacity was estimated with the Pitzer model:

$${}^{\phi}C_{p,\mathrm{NaCl(aq)}} + \frac{C^{\Theta}_{p,\mathrm{H_2O(l)}}}{n_r} = \frac{C_p\left(m_r\right)}{n_r} + \frac{\nu|z_{\mathrm{Na}}z_{\mathrm{Cl}}|A_{\mathrm{C}}}{2\mathrm{b}}\ln\left(\frac{1+\mathrm{b}\sqrt{I_m}}{1+\mathrm{b}\sqrt{I_r}}\right)$$
$$- 2\nu_{\mathrm{Na}}\nu_{\mathrm{Cl}}RT^2\left[\left(m-m_r\right)B^{C}_{\mathrm{NaCl}} + \left(m^2 - m_r^2\right)\nu_{\mathrm{Na}}z_{\mathrm{Na}}C^{C}_{\mathrm{NaCl}}\right] \qquad (46)$$

where m = molal concentration of the solute (mol kg–1)
n_r = amount of NaCl in reference solution (mol)
ν_{Na} = stoichiometric number of Na in NaCl (dimensionless)
ν_{Cl} = stoichiometric number of Cl in NaCl (dimensionless)
$\nu = \nu_{Na} + \nu_{Cl}$ (dimensionless)
$C_p(m_r)$ = constant-pressure heat capacity of a solution with a molality equal to m_r (J K^{-1} mol^{-1})
z_{Na} = charge number of the Na^+ cation (dimensionless)
z_{Cl} = charge number of the Cl^- anion (dimensionless)
A_C = Debye–Hückel coefficient for apparent molar constant-pressure heat capacity (J K^{-1} mol^{-1})
b = constant equal to 1.2 (kg$^{1/2}$ mol$^{-1/2}$)
I_m = molality-based ionic strength (mol kg^{-1})
I_r = molality-based ionic strength of the reference solution (mol kg^{-1}).

The quantities B^C_{NaCl} (kg K^{-2} mol^{-1}) and C^C_{NaCl} (kg^2 K^{-2} mol^{-2}) are defined by

$$B^C_{NaCl} = \left[\frac{\partial^2 \beta^{(0)}_{NaCl}}{\partial T^2}\right] + \frac{2}{T}\left[\frac{\partial \beta^{(0)}_{NaCl}}{\partial T}\right] + \left\{\left[\frac{\partial^2 \beta^{(1)}_{NaCl}}{\partial T^2}\right]_p + \frac{2}{T}\left[\frac{\partial \beta^{(1)}_{NaCl}}{\partial T}\right]_p\right\} \times \frac{1-\left(1+\alpha\sqrt{I_m}\right)\exp\left(-\alpha\sqrt{I_m}\right)}{\alpha^2 I_m} \quad (47)$$

and

$$C^C_{NaCl} = \left[\frac{\partial^2 C^{(0)}_{NaCl}}{\partial T^2}\right]_p + \frac{2}{T}\left[\frac{\partial C^{(0)}_{NaCl}}{\partial T}\right]_p + \left\{\left[\frac{\partial^2 C^{(1)}_{NaCl}}{\partial T^2}\right]_p + \frac{2}{T}\left[\frac{\partial C^{(1)}_{NaCl}}{\partial T}\right]_p\right\} \times \frac{6-\left(6+\alpha_2\sqrt{I_m}+3\alpha_2^2 I_m+\alpha_2^3 I_m \frac{3}{2}\right)\exp\left(-\alpha_2\sqrt{I_m}\right)}{\alpha_2^4 I_m^2} \quad (48)$$

where $\beta^{(0)}_{NaCl}$ and $\beta^{(1)}_{NaCl}$ are ion-interaction parameters of the Pitzer model (kg mol^{-1}); $C^{(0)}_{NaCl}$ and $C^{(1)}_{NaCl}$ are ion-interaction parameters of the Pitzer model (kg^2 mol^{-2}); α is a constant in the Pitzer model (= 2.0 kg$^{-1/2}$ mol$^{-1/2}$); and α_2 is a constant in the Pitzer model (as revised by Archer) (= 2.0 kg$^{-1/2}$ mol$^{-1/2}$). As can be inferred from eq 47 and 48, $\beta^{(0)}_{NaCl}$, $\beta^{(1)}_{NaCl}$, $C^{(0)}_{NaCl}$, and $C^{(1)}_{NaCl}$ are functions of T and p. Archer (1992) deveoped lengthy formulae to calculate these parameters.

Activity of H_2O. The activity of water, $a_{H_2O(l)}$, in an aqueous NaCl solution can be calculated by

$$a_{H_2O(l)} = \exp\left[-\phi_{H_2O(l)} \nu m_{NaCl(aq)}\right] \quad (49)$$

where $\phi_{H_2O(l)}$ is the osmotic coefficient of water (dimensionless) (Stokes 1991). The osmotic coefficient was calculated from the Pitzer model via

$$\left[\phi_{H_2O(l)} - 1\right] = -\left|z_{Na} z_{Cl}\right| A_\phi \frac{\sqrt{I_m}}{1 + b\sqrt{I_m}}$$
$$+ \; m \frac{2\nu_{Na}\nu_{Cl}}{\nu}\left[\beta^{(0)}_{NaCl} + \beta^{(1)}_{NaCl} \exp\left(-\alpha\sqrt{I_m}\right)\right]$$
$$+ \quad m^2 \frac{4\nu_{Na}{}^2\nu_{Cl}}{\nu}\left[C^{(0)}_{NaCl} + C^{(1)}_{NaCl} \exp\left(-\alpha_2\sqrt{I_m}\right)\right] . \qquad (50)$$

Activity of NaCl(aq). The mole-fraction-based activities (see App. A) that are called for by eq 41 are related to the molality-based activities typically calculated in solution chemistry by

$$\ln a_{x,B} = \ln a_{x,B} + \ln\left(M_A m^\ominus_B\right) \qquad (51)$$

where M_A is the molar mass of solvent A (kg mol^{-1}). The mean-ionic activity of NaCl(aq), $a_{\pm NaCl(aq)}$ (dimensionless) is calculated by

$$a_{\pm NaCl(aq)} = \frac{\gamma_{\pm NaCl(aq)} m_{\pm NaCl(aq)}}{m^\ominus_{\pm NaCl(aq)}} \qquad (52)$$

where $\gamma_{\pm NaCl(aq)}$ = mean-ionic activity coefficient of NaCl(aq) (dimensionless)
$m_{\pm NaCl(aq)}$ = mean-ionic molality of NaCl(aq) (mol kg^{-1})
$m^\ominus_{\pm NaCl(aq)}$ = standard-state mean-ionic molality of NaCl(aq) (mol kg^{-1}).

The mean-ionic activity coefficient, in turn, is calculated with the Pitzer model for a mean-ionic activity coefficient in a one-electrolyte aqueous solution:

$$\ln \gamma_\pm = -\left|z_{Na} z_{Cl}\right| A_\phi \left[\frac{\sqrt{I_m}}{1 + b\sqrt{I_m}} + \frac{2}{b}\ln\left(1 + b\sqrt{I_m}\right)\right]$$
$$+ \quad m \frac{2\nu_{Na}\nu_{Cl}}{\nu}\left\{2\beta^{(0)}_{NaCl} + \frac{\beta^{(1)}_{NaCl}}{\alpha_2 I_m}\left[1 - \left(1 + \alpha\sqrt{I_m} - \frac{\alpha^2 I_m}{2}\right)\exp\left(-\alpha\sqrt{I_m}\right)\right]\right\}$$
$$+ \quad m^2 \frac{4\nu_{Na}{}^2\nu_{Cl}}{\nu} \qquad (53)$$
$$\times \left[3C^{(0)}_{NaCl} + 4C^{(1)}_{NaCl} \frac{6 - \left(6 + 6\alpha_2\sqrt{I_m} + 3\alpha_2^2 I_m + 3\alpha_2^3 I_m^{3/2} - \frac{\alpha_2^4 I_m^2}{2}\right)\exp\left(-\alpha_2\sqrt{I_m}\right)}{\alpha_2^4 I_m{}^2}\right].$$

Temperature derivatives of the natural logarithms of activities of both $H_2O(l)$ and NaCl(aq). Temperature derivatives were calculated numerically. The derivative of a function f at T was estimated by a five-point numerical approximation,

$$f'(T_f) \approx \frac{1}{12\delta T}\left[f(T_f - 2\delta T) - 8f(T_f - \delta T) + 8f(T_f + \delta T) - f(T_f + 2\delta T)\right] \qquad (54)$$

where δT is a small increment chosen to be 0.1 K. The expected error of this estimate should be on the order of δT^4 (Burden and Faires 1989).

Molar volume of the liquid solution

The apparent molar volume NaCl(aq), ${}^{\phi}V_{\mathrm{NaCl(aq)}}$ (m^3 mol^{-1}), in a simple aqueous solution is

$$ {}^{\phi}V_{\mathrm{NaCl(aq)}} = \frac{V_{\mathrm{M}} - n_{\mathrm{H_2O(l)}} V^{\ominus}_{\mathrm{H_2O(l)}}}{n_{\mathrm{NaCl(aq)}}} \tag{55} $$

where ${}^{\phi}V_{\mathrm{NaCl(aq)}}$ = apparent molar volume of NaCl(aq) (m^3 mol^{-1})
V_{M} = actual solution volume (m^3 mol^{-1})
$V^{\ominus}_{\mathrm{H_2O(l)}}$ = standard-state molar volume of water (m^3 mol^{-1}).

The apparent molar volume of NaCl(aq) was calculated by

$$ {}^{\phi}V_{\mathrm{NaCl}} = \overline{V}^{\mathrm{o}}_{\mathrm{NaCl}} + \nu \left| z_{\mathrm{Na}} z_{\mathrm{Cl}} \right| \frac{A_V}{2b} \ln\left(1 + b\sqrt{I_m}\right) + 2\nu_{\mathrm{Na}}\nu_{\mathrm{Cl}} RT \left[m_{\mathrm{NaCl}} B^{\mathrm{V}}_{\mathrm{NaCl}} + m^2_{\mathrm{NaCl}} \left(\nu_{\mathrm{Na}} z_{\mathrm{Cl}}\right) C^{\mathrm{V}}_{\mathrm{NaCl}} \right] \tag{56} $$

where $\overline{V}^{\mathrm{o}}_{\mathrm{NaCl}}$ is the standard-state molar volume of NaCl (m^3 mol^{-1}) and A_V is the Debye–Hückel coefficient for apparent molar volume (m^3 $kg^{-1/2}$ $mol^{-1/2}$).

The quantities $B^{\mathrm{V}}_{\mathrm{NaCl}}$ and $C^{\mathrm{V}}_{\mathrm{NaCl}}$ (both kg Pa^{-1} mol^{-1}) are defined by

$$ B^{\mathrm{V}}_{\mathrm{NaCl}} = \left(\frac{\partial \beta^{(0)}_{\mathrm{NaCl}}}{\partial p} \right)_T + \left(\frac{\partial \beta^{(1)}_{\mathrm{NaCl}}}{\partial p} \right)_T \frac{\left[1 - \left(1 + 2\sqrt{I_m}\right)\exp\left(-2\sqrt{I_m}\right)\right]}{2I_m} \tag{57} $$

and

$$ C^{\mathrm{V}}_{\mathrm{NaCl}} = \left(\frac{\partial C_{\mathrm{NaCl}}}{\partial p} \right)_T = \frac{\left(\frac{\partial C^{\phi}_{\mathrm{NaCl}}}{\partial p} \right)_T}{2\left| z_{\mathrm{Na}} z_{\mathrm{Cl}} \right|^{1/2}}. \tag{58} $$

Temperature derivative of the solute chemical potential

The chemical potential of the solute can be restated in terms of its standard-state chemical potential, mean-ionic molality, and mean-ionic activity coefficient:

$$ \begin{aligned} \mu^{\mathrm{l}}_{\mathrm{NaCl}} &\equiv \mu_{\mathrm{NaCl(aq)}} \\ &= \mu^{\ominus}_{\mathrm{NaCl(aq)}} + RT \ln a_{\pm\mathrm{NaCl(aq)}} \\ &= \mu^{\ominus}_{\mathrm{NaCl(aq)}} + RT \ln\left[\frac{\gamma_{\pm\mathrm{NaCl(aq)}} m_{\pm\mathrm{NaCl(aq)}}}{m^{\ominus}_{\pm\mathrm{NaCl(aq)}}} \right] \end{aligned} \tag{59} $$

where $\mu^{\ominus}_{\mathrm{NaCl(aq)}}$ is the standard-state chemical potential of NaCl(aq) (J mol^{-1}) and $a_{\pm\mathrm{NaCl(aq)}}$ is the mean-ionic activity of NaCl(aq) (dimensionless). The temperature derivative of eq 59 was calculated numerically by eq 54.

Plots of capillary pressures against liquid specific volumes

The plots of the calculated ice-solution capillary pressures against the unfrozen-solution specific volumes are presented in the following figures. In general, these plots indicate that the relationship between capillary pressure and unfrozen solution volume was unaffected by the composition of the liquid phases.

The $p_c - V$ relationship for cooling of kaolinite pastes is presented in Figure 9. The general trend of the data points was a single line defining the $p_c - V$ relationship for this material. For the kaolinite pastes that were initially equilibrated with 0.1-mol kg^{-1} NaCl solutions, however, a pronounced deviation from this line was apparent at the lowest unfrozen solution contents. Similar deviations were found for some of the sand and montmorillonite pastes, but only for the pastes washed with 0.1-mol kg^{-1} NaCl solutions. This is apparently a systematic error, but we have been unable to determine its source. The warming curve for the kaolinite pastes is presented in Figure 10. No hysteresis was apparent when comparing the cooling and warming curves of these pastes, though here again there is an apparent systematic error in some of the data collected from the pastes washed with 0.1-mol kg^{-1} NaCl solutions.

The $p_c - V$ relationships for cooling and warming of montmorillonite pastes are presented in Figures 11 and 12, respectively. Unlike the kaolinite data, the general trend traced by the freezing curves for montmorillonite is much less smoothly curved than for kaolinite. In addition, there is far more scatter in the data. We believe that the abrupt decrease in specific volumes at higher capillary pressures is due to the large relative volume of liquid that was held in the interlamellar spaces of this clay—in these narrow spaces, capillary forces play a less significant role in maintaining the water unfrozen than does the so-called 'surface melting of the ice' (Brun et al. 1977, Dash 1989).

The $p_c - V$ relationships for cooling and warming of sand pastes are presented in Figures 13 and 14, respectively. As with montmorillonite, the general trend traced by the freezing curves of this clay is much less smoothly curved than for kaolinite. We believe that this abrupt transition is due to the coarse and fairly homogeneous pore-size distribution of these pastes, which allowed the solutions to freeze at higher and generally more uniform temperature.

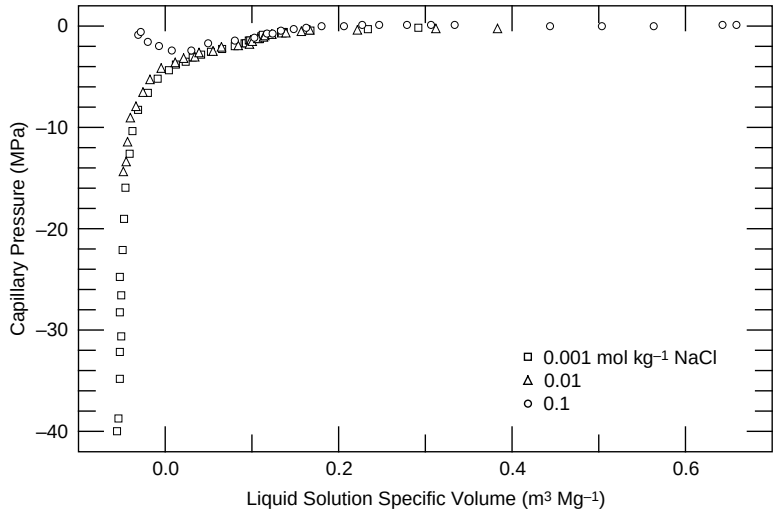

Figure 9. Relationships between unfrozen-solution specific volumes and ice-solution capillary pressures for kaolinite pastes cooled from 0°C to –66.6°C. The equilibrating solutions of the pastes were initially 0.1, 0.01, and 0.001 mol kg^{-1} NaCl.

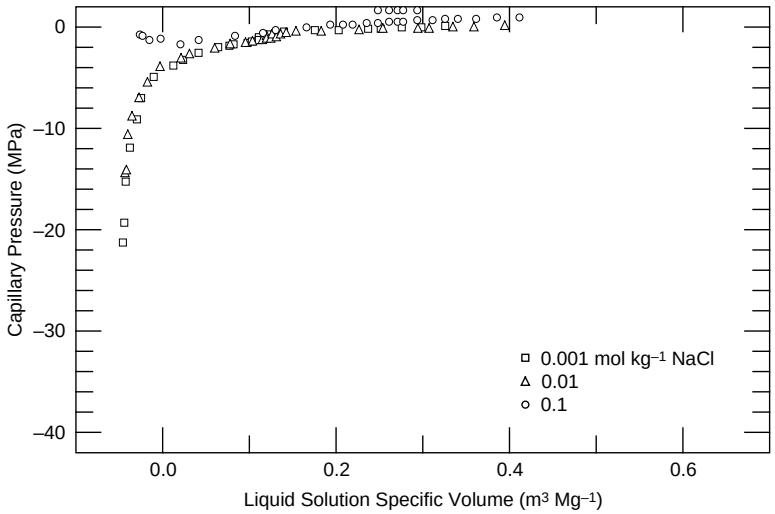

Figure 10. Relationships between unfrozen-solution specific volumes and ice-solution capillary pressures for kaolinite pastes warmed from –66.6°C to 0°C. The equilibrating solutions of the pastes were initially 0.1, 0.01, and 0.001 mol kg^{-1} NaCl.

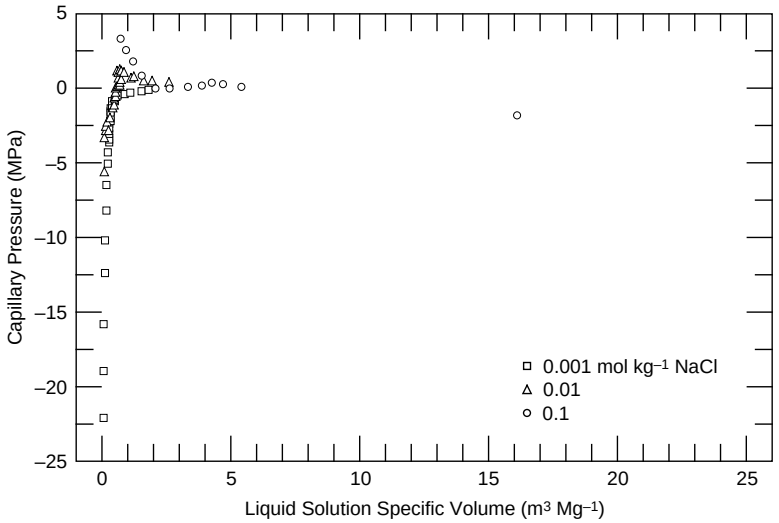

Figure 11. Relationships between unfrozen-solution specific volumes and ice-solution capillary pressures for montmorillonite pastes cooled from 0°C to –66.6°C. The equilibrating solutions of the pastes were initially 0.1, 0.01, and 0.001 mol kg^{-1} NaCl.

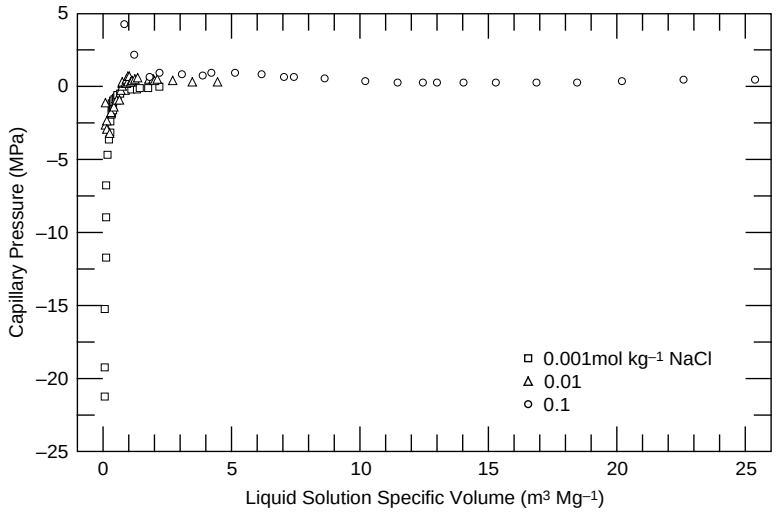

Figure 12. Relationships between unfrozen-solution specific volumes and ice-solution capillary pressures for montmorillonite pastes warmed from –66.6°C to 0°C. The equilibrating solutions of the pastes were initially 0.1, 0.01, and 0.001 mol kg^{-1} NaCl.

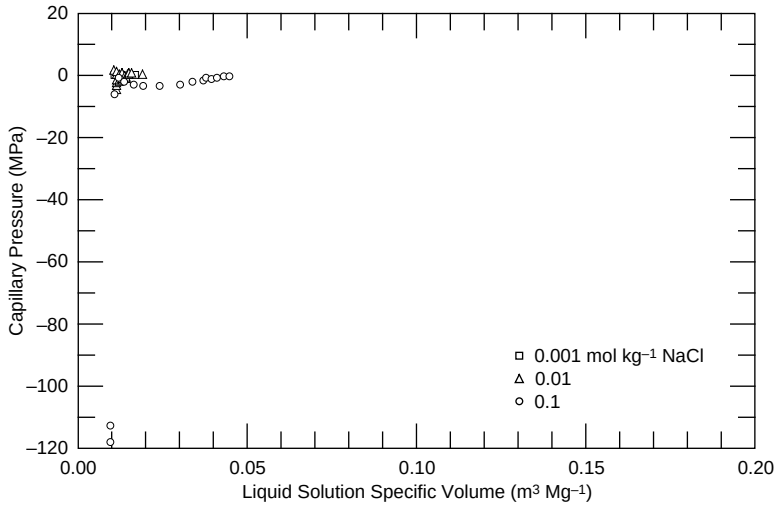

Figure 13. Relationships between unfrozen-solution specific volumes and ice-solution capillary pressures for sand pastes cooled from 0°C to –66.6°C. The equilibrating solutions of the pastes were initially 0.1, 0.01, and 0.001 mol kg^{-1} NaCl.

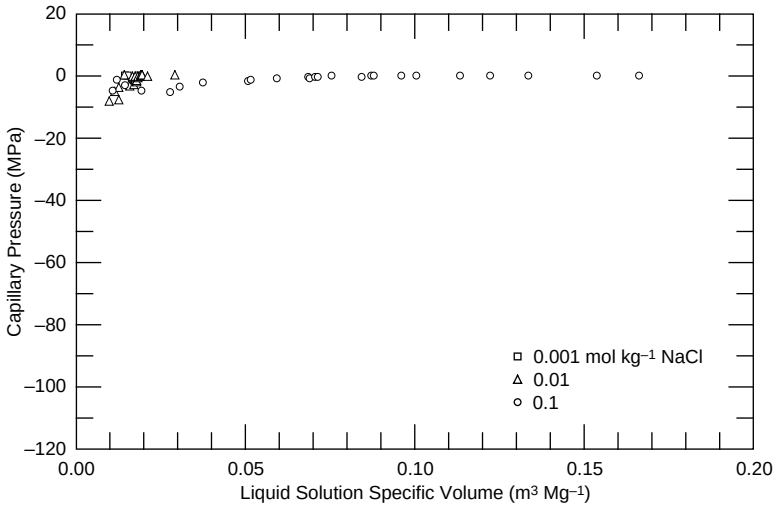

Figure 14. Relationships between unfrozen-solution specific volumes and ice-solution capillary pressures for sand pastes warmed from –66.6°C to 0°C. The equilibrating solutions of the pastes were initially 0.1, 0.01, and 0.001 mol kg^{-1} NaCl.

CONCLUSION

The minerals analyzed in this study may be thought to represent the range of applicability of capillary theory to explain the freezing behavior of porous solids. The kaolinite samples were not composed of an expanding-lattice clay with intermediate particle size, and the experimental results from this material supported the theory well. Sand and montmorillonite did not support it as well: sand because its particle size (and, therefore, pore radii) was too large, and montmorillonite because it has a much smaller particle size and because relatively large volumes of water can be held in its interlamellar spaces for which capillary forces are less important. Our study did indicate that capillarity theory coupled with the Pitzer model describes acceptably the effect of an electrolyte on the freezing curves of minerals of intermediate size between sand and montmorillonite.

LITERATURE CITED

Angell, C.A., J. Shuppert and J.C. Tucker (1973) Anomalous properties of supercooled water. Heat capacity, expansivity, and proton magnetic resonance chemical shift from 0 to –38°C. *Journal of Physical Chemistry*, **77:** 3092–3099.

Archer, D.G. (1992) Thermodynamic properties of the NaCl + H_2O system; 2: Thermodynamic properties of NaCl(aq), NaCl•$2H_2O$(cr), and phase equilibria. *Journal of Physical and Chemical Reference Data,* **21:** 793–829.

Atkins, P.W. (1990) *Physical Chemistry.* 4th edition. New York: W.H. Freeman and Co.

Bader, H. (1964) Density of ice as a function of temperature and stress. USA Cold Regions Research and Engineering Laboratory, Special Report 64.

Brun, M., A. Lallemand, J.-F. Quinson and C. Eyraud (1977) A new method for the simultaneous determination of the size and shape of pores, The thermoporometry. *Thermochimica Acta*, **21:** 59–88.

Butkovich, T.R. (1955) Density of single crystals from a temperate glacier. *Journal of Glaciology*, **2**(17): 553–559.

Burden, R.L. and J.D. Faires (1989) *Numerical Analysis*. 4th edition. Boston: PWS-KENT Publishing Co.
Chase, M.W. et al. (1985) JANAF thermochemical tables. 3rd edition. *Journal of Physical and Chemical Reference Data*, vol. 14, supplement 1, pp. 1–1856.
Dash, J.G. (1989) Thermomolecular pressure in surface melting: Motivation for frost heave. *Science*, **246**(4937): 1591–1593.
Defay, R. and I. Prigogine (1966) *Surface Tension and Adsorption*. Translated by D.H. Everett. London: Longmans.
Dorsey, N.E. (1940) *Properties of Ordinary Water Substance.* American Chemical Society. New York: Reinhold.
Evans, R. and U.M.B. Marconi (1986) Fluids in narrow pores: Adsorption, capillary condensation and critical points. *Journal of Chemical Physics*, **84:** 2376–2399.
Everett, D.H. (1961) The thermodynamics of frost damage to porous solids. *Journal of the Chemical Society, Faraday Transactions*, **57**(9): 1541-1551.
Giauque, W.F. and J.W. Stout (1936) The entropy of water and the third law of thermodynamics; The heat capacity of ice from 15 to 273°K. *Journal of the American Chemical Society*, **58:** 1144–1150.
Haida, O., T. Matsuo, H. Suga and S. Seki (1974) Calorimetric study of the glassy state, 10: Enthalpy relaxation at the glass transition temperature of hexagonal ice. *Journal of Chemical Thermodynamics*, **6:** 815–825.
Handa, Y.P., R.E. Hawkins and J.J. Murray (1984) Calibration and testing of a Tian–Calvet heat-flow calorimeter: Enthalpies of fusion and heat capacities for ice and tetrahydrofuran hydrate in the range 85 to 270 K. *Journal of Chemical Thermodynamics*, **16**(7): 623–6732.
Hare, D.E. and C.M. Sorensen (1987) The density of supercooled water, II: Bulk samples cooled to the homogeneous nucleation limit. *Journal of Chemical Physics*, **87:** 4840–4845.
Hill, P.G. (1990) A unified equation of state for H_2O. *Journal of Physical and Chemical Reference Data*, **19:** 1231.
Hobbs, P.V. (1974) *Ice Physics.* Oxford: Clarendon Press.
Ketcham, W.M. and P.V. Hobbs (1969) An experimental determination of the surface energies of ice. *Philosophical Magazine*, **19**(162): 1161–1173.
LaPlaca, S. and B. Post (1961) Thermal expansion of ice. *Acta Crystallographica*, **13:** 503–505.
Lonsdale, K. (1958) The structure of ice. *Proceedings of the Royal Society (London)*, **247A**: 424–434.
Lupis, C.H.P. (1983) *Chemical Thermodynamics of Materials.* New York: North–Holland.
Maier, C.G. and K.K. Kelley (1932) An equation for the representation of high-temperature heat content data. *Journal of the American Chemical Society*, **54:** 3243–3246.
Marion, G.M. and S.A. Grant (1994) FREZCHEM, A chemical–thermodynamic model for aqueous solutions at subzero temperatures. USA Cold Regions Research and Engineering Laboratory, Special Report 94-18.
Mills, I. (1988) Quantities, units, and symbols in physical chemistry. International Union of Pure and Applied Chemistry (IUPAC). Osney Mead, Oxford: Blackwell Scientific Publications.
Pitzer, K.S. (1991) Ion interaction approach, Theory and data collection. In *Activity Coefficients in Electrolyte Solutions* (K.S. Pitzer, Ed.), 2nd edition. Boca Raton, Florida: CRC Press.
SAS Institute (1985) *SAS® User's Guide, Statistics.* Version 5 edition. Cary, North Carolina: SAS Institute, Inc.
Spencer, R.J., N. Møller and J.H. Weare (1990) The prediction of mineral solubilites in natural waters, A chemical equilibrium model for the Na–K–Ca–Mg–Cl–

SO_4–H_2O system at temperatures below 25°C. *Geochimica et Cosmochimica Acta,* **54:** 575–590.

Speedy, R.J. (1987) Thermodynamic properties of supercooled water at 1 atm. *Journal of Physical Chemistry*, **91:** 3354–3358.

Stokes, R.H. (1991) Thermodynamics of solutions. In *Activity Coefficients in Electrolyte Solutions* (K.S. Pitzer, Ed.), 2nd edition. Boca Raton, Florida: CRC Press.

Taylor, B.N. and E.R. Cohen (1990) Recommended values of the fundamental physical constants, a status report. *Journal of Research, National Institute of Standards Technology*, **95:** 497.

Tice, A.R., D.M. Anderson and K.F. Sterrett (1981) Unfrozen water contents of submarine permafrost determined by nuclear magnetic resonance. *Engineering Geology*, **18:** 135–146.

Tice, A.R., J.L. Oliphant, Y. Nakano and T.F. Jenkins (1982) Relationship between the ice and unfrozen water phases in frozen soil as determined by pulsed nuclear magnetic resonance and physical desorption data. USA Cold Regions Research and Engineering Laboratory, CRREL Report 82-15.

APPENDIX A: EFFECT OF CONCENTRATION SCALES ON ACTIVITIES

The value of an activity of a solute depends on the concentration scale that is chosen. This is because the standard-state chemical potentials for different reference functions are themselves different (Mills 1988). For a molality reference function, the standard-state chemical potential for solute B is

$$\mu^{\ominus}_{m,\mathrm{B}}(T) = \left[\mu\left(T, p^{\ominus}, m_{\mathrm{B},\ldots}\right) - RT\ln\left(\frac{m_{\mathrm{B}}}{m^{\ominus}_{\mathrm{B}}}\right)\right]^{\infty} \tag{60}$$

and the standard-state chemical potential for solute B for a mole-fraction reference function is

$$\mu^{\ominus}_{x,\mathrm{B}}(T) = \left[\mu\left(T, p^{\ominus}, m_{\mathrm{B},\ldots}\right) - RT\ln\left(x_{\mathrm{B}}\right)\right]^{\infty}. \tag{61}$$

Subtracting eq 60 from eq 61 yields

$$\mu^{\ominus}_{x,\mathrm{B}}(T) - \mu^{\ominus}_{m,\mathrm{B}}(T) = -RT\left[\ln\left(x_{\mathrm{B}}\right) - \ln\left(\frac{m_{\mathrm{B}}}{m^{\ominus}_{\mathrm{B}}}\right)\right]^{\infty}. \tag{62}$$

This is equivalent to

$$\mu^{\ominus}_{x,\mathrm{B}}(T) - \mu^{\ominus}_{m,\mathrm{B}}(T) = -RT\left[\ln\left(\frac{m_{\mathrm{B}}}{\frac{1}{M_{\mathrm{A}}} + m_{\mathrm{B}}}\right) - \ln\left(\frac{m_{\mathrm{B}}}{m^{\ominus}_{\mathrm{B}}}\right)\right]^{\infty} \tag{63}$$

and

$$\mu^{\ominus}_{x,\mathrm{B}}(T) - \mu^{\ominus}_{m,\mathrm{B}}(T) = -RT\left[\ln\left(\frac{\frac{m_{\mathrm{B}}}{m^{\ominus}_{\mathrm{B}}}}{\frac{\frac{1}{M_{\mathrm{A}}} + m_{\mathrm{B}}}{m^{\ominus}_{\mathrm{B}}}}\right) - \ln\left(\frac{m_{\mathrm{B}}}{m^{\ominus}_{\mathrm{B}}}\right)\right]^{\infty} \tag{64}$$

which results in

$$\mu^{\ominus}_{x,\mathrm{B}}(T) = \mu^{\ominus}_{m,\mathrm{B}}(T) - RT\ln\left(M_{\mathrm{A}} m^{\ominus}_{\mathrm{B}}\right). \tag{65}$$

The molality-based activity of solute B is

$$a_{m,\mathrm{B}} = \exp\left[\frac{\mu_{\mathrm{B}} - \mu^{\ominus}_{m,\mathrm{B}}}{RT}\right] \tag{66}$$

and its mole-fraction-based activity is

$$a_{x,\mathrm{B}} = \exp\left[\frac{\mu_{\mathrm{B}} - \mu^{\ominus}_{x,\mathrm{B}}}{RT}\right]. \tag{67}$$

One can derive immediately

$$\ln a_{x,\mathrm{B}} = \ln a_{m,\mathrm{B}} + \ln\left(M_{\mathrm{A}} m_{\mathrm{B}}^{\ominus}\right). \tag{68}$$

REPORT DOCUMENTATION PAGE

Form Approved
OMB No. 0704-0188

1. AGENCY USE ONLY (Leave blank)	2. REPORT DATE	3. REPORT TYPE AND DATES COVERED
	January 1999	

4. TITLE AND SUBTITLE
Effect of Dissolved NaCl on Freezing Curves of Kaolinite, Montmorillonite, and Sand Pastes

5. FUNDING NUMBERS
WU: F02
DE-AI05-940R22141
4A161102AT24

6. AUTHORS
S.A. Grant, G.E. Boitnott, and A.R. Tice

7. PERFORMING ORGANIZATION NAME(S) AND ADDRESS(ES)
U.S. Army Cold Regions Research and Engineering Laboratory
72 Lyme Road
Hanover, New Hampshire 03755

8. PERFORMING ORGANIZATION REPORT NUMBER
Special Report 99-2

9. SPONSORING/MONITORING AGENCY NAME(S) AND ADDRESS(ES)
Office of the Chief of Engineers
Washington, DC 20314-1000

Strategic Environmental Research and Development Program
Arlington, Virginia 22203

Department of Energy
Washington, DC 20585

10. SPONSORING/MONITORING AGENCY REPORT NUMBER

11. SUPPLEMENTARY NOTES

12a. DISTRIBUTION/AVAILABILITY STATEMENT
Approved for public release; distribution is unlimited.
Available from NTIS, Springfield, Virginia 22161

12b. DISTRIBUTION CODE

13. ABSTRACT (*Maximum 200 words*)

We developed a chemical-thermodynamic procedure for calculating the capillary pressures of aqueous NaCl solutions in a porous medium at temperatures below 0°C by extending the treatment by Brun et al. (1977). Ice in the porous medium was assumed to be a pure phase with thermophysical properties identical to bulk hexagonal ice. The thermophysical properties (and the attendant derivative and integral properties) of the electrolyte solutions were calculated with the Pitzer model as parameterized by Archer (1992).

Experiments were conducted to test this procedure. Pastes of kaolinite clay, montmorillonite, and quartz sand were prepared by washing repeatedly with aqueous solutions of 0.1-, 0.01-, and 0.001-mol kg^{-1} NaCl. The molar unfrozen water contents of these pastes were measured by pulsed nuclear magnetic resonance (NMR) in the temperature range –0.14°C to –66.6°C.

The relationships between ice-solution capillary pressures and specific solution volumes for frozen pastes of each mineral were plotted for all initial solution molalities. While some systemic errors were evident, these plots indicated that the capillary pressure-volume relationships were consistent for pastes of the three minerals and, as expected from theory, unaffected by initial equilibrating solution molality.

14. SUBJECT TERMS	15. NUMBER OF PAGES
Frozen ground Sodium chloride Soil freezing curve	39
	16. PRICE CODE

17. SECURITY CLASSIFICATION OF REPORT	18. SECURITY CLASSIFICATION OF THIS PAGE	19. SECURITY CLASSIFICATION OF ABSTRACT	20. LIMITATION OF ABSTRACT
UNCLASSIFIED	UNCLASSIFIED	UNCLASSIFIED	UL